Determination of geomembrane - protective geotextile friction angle: an insight into the shear rate effect

G. Stoltz, Sylvie Nicaise, G. Veylon, D. Poulain

Determination of geomembrane – protective geotextile friction angle: an insight into the shear rate effect

Guillaume Stoltz[1](*), Sylvie Nicaise[2], Guillaume Veylon[3], Daniel Poulain[4]

1 Irstea – Aix Marseille Univ, RECOVER Unit, 3275 Route Cézanne,13182 Aix-en-Provence, France, Email: guillaume.stoltz@irstea.fr , Phone number: +33442666964

2 Irstea – Aix Marseille Univ, RECOVER Unit, 3275 Route Cézanne,13182 Aix-en-Provence, France, Email: sylvie.nicaise@irstea.fr , Phone number: +33442669954

3 Irstea – Aix Marseille Univ, RECOVER Unit, 3275 Route Cézanne,13182 Aix-en-Provence, France, Email: guillaume.veylon@irstea.fr , Phone number: +33442667936

4 Irstea – Aix Marseille Univ, RECOVER Unit, 3275 Route Cézanne,13182 Aix-en-Provence, France, Email: daniel.poulain@irstea.fr , Phone number: +33442666964

(*) Corresponding author : Dr. Guillaume Stoltz, Engineer of Research, Irstea – Aix Marseille Univ, RECOVER Unit, 3275 Route Cézanne,13182 Aix-en-Provence Cedex 5, France, Email: guillaume.stoltz@irstea.fr , Phone number: +33442666964

Abstract

This study investigates how the shear rate can affect the geomembrane – protective geotextile friction angle. Four types of geomembranes (GMB) were considered (EPDM, HPDE, PP, and PVC) and a single nonwoven needle-punched geotextile (GTX_{nw}) was used to make the interfaces with the geomembrane. Three shear devices were used: a large-scale inclined plane (IP), a shear box (SB), and a small-scale shear device (ssSD). The ssSD allows two shear modes to be compared: one mode involves incrementally increasing the shear stress, and the other involves imposing a constant tangential velocity at the interface. Only the PP GMB- GTX_{nw} was tested with the SB and the ssSD. Inclined plane standardised tests show that for the three interfaces that undergoes gradual sliding (EPDM, PP and PVC GMB- GTX_{nw}), it is shown that a step-by-step experimental procedure gives significantly lower interface friction angle than that given by the procedure from the current international standard, which is explained by the increase of interface shear stress with sliding speed. These observations are confirmed by shear box tests. One major practical result is that, following the nature of geosynthetics, the shear rate applied in large-scale shear box tests should be adapted to assess a safety value of a geosynthetic - geosynthetic interface friction angle.

Keywords: geosynthetic, geomembrane lining system, friction angle, inclined plane, shear box.

1. Introduction

1.1 Assessing the stability of geosynthetics lining systems

Geomembrane lining systems (GLSs) are widely used in earthfill dams, hydraulics ponds and landfills, where they are typically protected by a layer of earth or gravel. Several geosynthetics are usually combined to provide the desired functions (waterproofing, drainage, resistance to puncturing, ...), so the stability of the protective layer (i.e., the granular materials spread over the GLSs) depends strongly on the characteristics of the interfaces between geosynthetics and at the geosynthetic-soil interface. In particular, the geosynthetic-geomembrane interface often has a relatively low friction angle. Various methods are available to calculate the stability against translational failure of such GLSs so that, if required, a reinforcing geosynthetic to be anchored at the top of the slope can be designed. These methods fall into two categories: (i) analytical limit equilibrium methods (Giroud and Beech, 1989; Koerner and Hwu, 1991), such as methods used to analyse infinite slopes (see, e.g., Martin and Koerner, 1985; Thiel, 1998) or finite slopes with two-part wedges (see, e.g., Giroud et al., 1995, Koerner and Soong, 2000), and (ii) numerical modelling methods (Fowmes et al., 2008; Tano et al., 2016; Tano et al., 2017a). Lastly, although complex to implement, experimental methods to assess the stability of actual earthworks, using, for example, real-scale physical modelling or centrifuge simulations, are possible.

1.2 Assessment of interface shear resistance

To guarantee the stability and durability of GLSs over decades and avoid failure, the determination of all interfaces shear resistances is a major issue in GLS design, in particular for GLSs on slopes with a thin overlying soil layer, as evinced by Stark et al. (2008) from a back-analysis of a PVC geomembrane-lined pond failure. In GLSs, geomembranes are often in contact with an overlying and/or underlying gravel layer (that provide drainage, for example). To protect the geomembrane from being damaged by stones due to normal loading and also static, monotonic, or cyclic shear

loading (Fox et al., 2011; Fox et al., 2014; Fox and Thielmann, 2014), protective nonwoven needle-punched geotextiles are generally placed between the geomembrane and the soil or gravel layer. In GLSs with a smooth geomembrane, the geomembrane – protective geotextile interface typically has the lowest friction angle (i.e., shear resistance). Thus, to ensure the proper design of a reinforcing geosynthetics, the GLS stability on a slope may be evaluated based on this parameter. Depending on the situation, the GLS stability versus dynamic loading, induced in most cases by earthquake, has to be ensured.

The shear resistance at interfaces involving geosynthetics may be affected by numerous parameters that affect the mechanical behaviour of such interfaces; for example, the normal stress (Bacas et al., 2015a; Kim and Frost, 2011), moisture content (Ferreira et al., 2015; Lopes et al., 2014), dynamic conditions (De and Zimmie, 1998; Kim et al., 2005; Pavanello et al., 2018a; Pavanello et al., 2018b; Yegian and Kadakal, 1998; Yegian and Lahlaf, 1992) temperature (Frost and Karademir, 2016; Hanson et al., 2015; Yesiller et al., 2016), geomembrane surface roughness (Bacas et al., 2015b; Hebeler et al., 2005; Frost and Lee, 2001) and sliding history (Stoltz and Vidal, 2013; Zettler et al., 2000), including cyclic shear loading (Fox et al., 2011; Vieira et al., 2013). Concerning the constitutive mechanical failure criterion, several studies evinced a linear failure envelope for smooth HDPE geomembrane/nonwoven needle-punched geotextile interfaces (see, for example, Stark and Poeppel, 1994; Stark et al., 1996) and for smooth PVC geomembrane/geotextile interfaces (Hillman and Stark, 2001). However, some types of geomembrane/geotextile interfaces exhibit nonlinear failure envelopes; for example, Stark et al. (1996) observed this behaviour for textured HDPE geomembrane/nonwoven geotextile interfaces.

In addition to the interface shear resistance, another relevant mechanical characteristic that is not often used or discussed is the displacement of the interface, which leads to the maximal shear resistance and from which the peak friction angle is calculated. This parameter, which may be called “peak displacement” (Fowmes et al., 2008), is linked to the interface shear stiffness which in turn is a

useful parameter to numerically model the mechanical behaviour of geosynthetic interfaces (Tano et al., 2016).

Overall, interface shear resistance is related to the two materials in contact, which may be two geosynthetics or a soil and a geosynthetic. The main parameter that characterises the interface shear resistance is the friction angle, which can be measured by using the direct shear box (SB) test as per the standard EN ISO 12957-1 or by using the inclined plane (IP) test as per the standard EN ISO 12957-2. In the SB test, the normal stress applied ranges from 50 to 150 kPa whereas, in the IP test, the normal stress applied is 5 kPa. The SB test is thus more suitable for interfaces subjected to high stress (lateral and bottom barriers) whereas the IP test is more suitable for designing a thin soil layer to be applied on a sloped multi-layer geosynthetic. Alternatively, some other apparatus can be used, such as, for example, a ring shear device (Stark and Poeppel, 1994; Stark et al., 1996), which can be used over a relatively large range of normal stress (for example, from 17 to 400 kPa; see Hillman and Stark, 2001).

In addition, these two tests have different loading procedures: for the SB test, the tested interface is loaded by increasing displacement at a controlled rate whereas, for the IP test, the tested interface is loaded by increasing shear stress at a controlled rate.

Although previous studies (Reyes Ramirez and Gourc, 2003; Wasti and Özdüzgün, 2001) have compared the results of IP and SB tests, the comparison may be biased because of the various normal stresses of each test and the means by which they were applied: directly by soil weight for the IP device and typically with a jack for the SB device. In addition, the various types and sizes of experimental devices that may be used may also distort the comparisons, primarily because of various “edge effects”, as shown by Stoltz and Hérault (2014) who compared results from IP and SB tests done under the same testing conditions (i.e., normal stress and method used to apply this stress, sample size, upper box of the device, etc.).

The IP test has been extensively studied and consists of increasing the shear stress until the tested geosynthetics interfaces begins to slide (Briançon et al., 2002; Koutsourais et al., 1991; Palmeira et al., 2002). However, recent studies have indicated that the standardised testing procedure for the IP test, requiring a relative displacement of 50 mm, may give a nonconservative measurement of the friction angle. In fact, Reyes Ramirez and Gourc (2003) showed that the standardised testing procedure for the IP test gives the (standardised) friction angle based on a static analysis for conditions that are actually dynamic. Thus, Reyes Ramirez and Gourc (2003) warn that the standardised procedure can overestimate the friction angle of interfaces involving geosynthetics. Pitanga et al. (2009) showed that the friction angle corresponding to the initiation of sliding and the friction angle corresponding to sliding at constant acceleration are generally smaller than the standardised friction angle. However, they did not conclude on the friction angle that should be used in designing GLSs. Briançon et al. (2011) developed a modified procedure for the IP device called the "force procedure". By using this procedure, they obtained smaller friction angles than when using the standardised testing procedure for the IP test. Stoltz et al. (2012) proposed another procedure, closely related to the force procedure of Briançon et al. (2011), in which the upper box is retained by a deformable element, thereby controlling the sliding of the upper box while measuring the force required to retain it. This testing procedure allows the interface friction forces to be assessed during the entire slide of the interface. More recently, Carbone et al. (2015) proposed the "unified inclined-plane procedure" to determine the static and dynamic interface friction angles.

Thus, the complex and varying mechanical behaviour of interfaces involving geosynthetics has led to the devolvement of various testing procedures for IP devices. A common thread in all these efforts to improve the testing procedure for the IP test is that the current standard does not allow the post-peak interface friction angle to be assessed for safety mechanical numerical modellings of the multilayer geosynthetics used in geostructures.

Regarding the SB test, which involves imposing a displacement at a constant rate on a GSY interface, it can determine the interface friction angle also at post-peak condition, even if only the peak friction angle is considered by the standard EN ISO 12957-1. Moreover, Stoltz and Auray (2014) showed that the maximal displacement of 50 mm given in the standard is insufficient for some tested interfaces, such as a sand-geogrid interface, where the insufficient displacement prevents the interface friction angle from being determined at large displacements, with the geogrid in full traction. In addition, although the relative displacement of the interface at maximal shear resistance could also be determined, the standard EN ISO 12957-1 gives no procedure to do so.

A partial conclusion is thus that no current standard describes how to obtain all requisite parameters for the interface shear resistance (interface friction angle at small and large displacements and over a wide range of normal stress and relative displacement at the interface at maximal shear resistance) required for a reliable analytical limit equilibrium analysis or for the more complex mechanical numerical modelling of geosynthetic multi-layers in geostructures. Thus, significant work is required to improve the current standards so that geosynthetic characteristics may be reliably and reproducibly determined under actual field conditions (i.e., hydraulic conditions, thermal conditions, etc.).

The present study thus uses three experimental devices to investigate the effect of interface sliding speed/shear rate on the determination of smooth geomembranes / protective geotextile interface friction angle: a small-scale shear box that can apply shear by force or by displacement at a given contact rate, a large-scale inclined plane and a large-scale shear box. The present study compares the interface shear strength measured with various devices and following different testing procedures; in particular with a varying rate of displacement. However, some results are presented in terms of friction angle to facilitate communication with a large community of engineers and researchers. Therefore, to assess the friction angle from the measured shear resistance, a secant friction angle for IP test and a linear failure envelope for SB and ssSD test are considered for all the interfaces tested.

2. Methods and Materials

2.1. Experimental devices

This section presents the experimental devices used in this study and the methods and assumptions used to calculate the results.

2.1.1. Large-scale inclined plane

The IP device is an inclinable plane on which an upper box with wheels can move along rails on either side of the plane. The upper box is 1 m long and 1 m wide (Figure 1). Details of the apparatus that was used in this study can be found in Briançon et al. (2002). The plane inclination β (or β_{IP} in the graphs) can be fixed at a desired value or increased at a constant rate (Figure 2). To test a soil-geosynthetic interface, the geosynthetic is anchored to the backside of the plane and the upper box is filled with the soil to be tested (see Figure 1). To test a geosynthetic-geosynthetic interface, the lower geosynthetic is anchored to the backside of the plane and the upper geosynthetic is anchored to the front side of the upper box, which is filled with a standardised sand to impose a given normal stress (a relatively low stress; i.e., generally less than 10 kPa). In any case, the support of the lower geosynthetic being tested must have a high-friction surface to avoid any traction effort in the geosynthetics. The surface of the device is covered by a P80 abrasive sheet.

When the inclination of the plane β is increased at a constant rate $d\beta/dt$ (Figure 2), the shear stress τ_{IP}, which acts at the interface and is due to the weight of the inclined soil, increases follows:

$$\tau_{IP}(\beta) = \sigma_0 \sin(\beta) + f_r(\beta)/A \quad (1)$$

where σ_0 is the initial normal stress (for β = 0°), fr(β) is the resulting force required to hold back the empty upper box and A the contact area.

While τ_{IP} increases, the normal stress σ_{IP} decreases as follows:

$$\sigma_{IP}(\beta) = \sigma_0 \cos(\beta) \quad (2)$$

where σ_0 is the initial normal stress (for $\beta = 0°$).

The loading method consists of imposing a shear force at the interface, and the response is measured in terms of relative tangential displacement δ_{IP}. Following this type of test, before the plane inclination denoted β_{is} (that is β at initial sliding, superior to zero) the upper and lower layers of the interface to be tested are stationary (Figure 2). Overcoming the plane inclination β_{is}, the upper box will slide at a speed that depends on the materials being tested. When the upper box is sliding, the interface shear stress τ_{IP}, which is approximated by equation (1), is derived from the free-body diagram (Figure 2) for static conditions. In other words, any possible force that accelerates the upper box is not taken into account. The interface shear resistance, and thus its friction angle in the typical case of a Mohr-Coulomb failure criterion, depends on the inclination of the plane at the interface failure.

Depending on the interface being tested, the curve of the measured tangential displacement δ_{IP} as a function of plane inclination β will fall into two general categories, even if other intermediate ways of sliding may occur (Figure 3a):

(i) A “sudden-sliding” curve corresponds to the upper box remaining stable until the plane inclination reaches β_{is}, after which the upper box accelerates. In this situation, the acceleration measurement is required to determine the post-peak friction angle.

(ii) A “gradual-sliding” curve corresponds to a progressive sliding of the upper box at low speed (quasi-static conditions). In this case, the acceleration may be neglected and no well-defined failure of the tested interface exists. In other words, the curve does not allow the shear strength to be clearly identified.

The standard EN ISO 12957-2 describes a testing procedure that uses an IP device and standardises the plane inclination to give a value for the friction angle of the interface being tested. In this standard, the initial normal stress σ_0 is 5.0 ± 0.1 kPa and the rate of plane inclination is $d\beta/dt$ = 3.0°±0.5°/min. The standardised friction angle φ_{50} of the tested interface is calculated based on the

measured plane inclination β_{50}, which corresponds to the measured plane inclination when the upper box slides a tangential displacement δ_{50} of 50 mm. Thus,

$$\tan\varphi_{50} = \frac{\sigma_0 \sin(\beta_{50}) + f_r(\beta_{50})/A}{\sigma_0 \cos(\beta_{50})} \quad (3)$$

where fr(β_{50}) is the force required to restrain the empty upper box when δ_{50} = 50 mm.

When the tangential displacement exceeds 50 mm, the upper box is restrained by a chain that stops the test.

The test is repeated on three interfaces, with virgin specimens and at the same normal stress of 5 kPa, and the friction angle is determined from the mean of the three measurements. Note that the standard EN ISO 12957-2 only considers secant friction angle at σ_n = 5 kPa [i.e., equation (3) independent of normal stress] without any cohesion or adhesion [i.e., the Mohr-Coulomb failure criterion is a straight line passing through zero in the (σ_n, τ) diagram].

In addition to doing inclined plane tests following the standardised procedure of EN ISO 12957-2, other tests can be done by changing various conditions. In particular, this is the case for the method that increases the plane inclination, which can be done incrementally. This method was applied in this study by increasing the plane inclination, step by step, in 1° increments per hour. In this procedure, tangential displacement was monitored during the entire test by using a Gefran PC rectilinear displacement transducer (independent linearity ±0.05%) linked to a PCI-6229 data acquisition card from National Instruments. The plane inclination rate to reach each step was 3°/min. Given this incremental testing procedure, the method by which the interface friction angle was determined and the measurement accuracy must be clarified. For a given plane inclination β, the upper box may be stable and, for the following β+1°, the upper box may undergo continuous sliding. Thus, the selection of β, or β+1°, to determine the interface friction angle is questionable. According to the standardised testing procedure, the friction angle should be determined when the upper box is sliding (i.e., from β+1° in the above example) whereas the safest approach would have determined

the friction angle at the step just before sliding (i.e., from β). In this study, the friction angle was determined by using the incremental testing procedure from the middle plane inclination between the steady state and slipping state [i.e., (β+β+1)/2]. Thus, unlike the standardised testing procedure, for which the friction angle uncertainty was about ±0.2° (derived from the sensors uncertainty and the maximal error of the inclination of the two rails that support the upper box), in the incremental testing procedure with plane inclination step of 1°, the friction angle was determined with an uncertainty of ±0.7°.

2.1.2. Large-scale shear box

The large-scale SB device consists of a horizontal plane on which is placed an upper mobile box that is displaced at constant velocity by a hydraulic jack. The upper box is 0.3 m long and 0.3 m wide (Figure 1). To test a soil-geosynthetic interface, the geosynthetic is anchored on the horizontal plane, underneath the upper box, which is filled with the soil to be tested and loaded by a vertical jack to create a relatively high normal stress (i.e., generally greater than 50 kPa). More details about this testing procedure are available in Tano et al. (2017b). To test a geosynthetic-geosynthetic interface, the upper geosynthetic is put in the upper box in a U shape and then filled with a standardised sand and loaded by a vertical jack. Similar to the requirement of the IP device, the support of the lower geosynthetic in the SB test must have a high-friction surface to avoid any traction effort in the geosynthetic, so the surface is covered by a P80 abrasive sheet. As opposed to the IP device, the SB test consists of imposing on the interface a tangential displacement at constant velocity while simultaneously recording the shear stress τ_{SB} at the interface by means of a force sensor (Figure 2b). In this situation, the normal stress is held constant during the entire shear test.

Depending on the interface and on the level of normal stress, the measured shear stress τ_{SB} as a function of tangential displacement δ_{SB} can take on one of two typical forms (Figure 3b): a peak-plateau shear form (also called strain softening) or a single-plateau shear form. In the former case, in

which the shear curve exhibits a peak followed by a plateau, two friction angles can be determined: a peak friction angle φ_{SBpeak} [equation (4)] and a post-peak friction $\varphi_{SBp\text{-}peak}$ angle [equation (5)]:

$$\tan\varphi_{\mathrm{SBpeak}} = \frac{\tau_{\mathrm{SBpeak}}}{\sigma_n}\,(c_{\mathrm{interface}} = 0) \tag{4}$$

$$\tan\varphi_{\mathrm{SBp-peak}} = \frac{\tau_{\mathrm{SBp-peak}}}{\sigma_n}\,(c_{\mathrm{interface}} = 0) \tag{5}$$

where τ_{SBpeak} is the maximum shear stress of the curve (δ_{SB}, τ_{SB}), $\tau_{SBp\text{-}peak}$ (τ_{res} in Fig 3b) is the plateau of the curve (δ_{SB}, τ_{SB}) and σ_n is the normal stress. Equations (4) and (5) are derived from the Mohr-Coulomb failure criterion with no cohesion or adhesion, i.e. a linear failure envelope is assumed.

The interface friction angle is a mechanical characteristic that is destined for use in the design of geostructures, especially including GLSs. For design, whether to use the peak friction angle φ_{SBpeak} or the post-peak friction $\varphi_{SBp\text{-}peak}$ is a relevant question for engineers [see the in-depth analysis of Stark and Choi (2004)].

The standard EN ISO 12957-1 (last revised version published in 2018) provides a testing procedure involving a large-scale SB device to determine the friction angle at soil-geosynthetic or geosynthetic-geosynthetic interfaces under high normal stress (between 50 and 150 kPa). The standard uses a displacement rate of δ_{SB}/dt = 1 mm/min and describes only how to determine the peak friction angle. Unlike the standard EN ISO 12957-2, in the standard EN ISO 12957-1, the best fit regression straight line corresponding to the Mohr-Coulomb failure criterion in the (σ_n, τ) diagram does not necessarily pass through zero, so an apparent adhesion can be obtained from the test on geosynthetic-geosynthetic interface. However, to make comparisons in the present study, no apparent adhesion is considered for the large-scale SB test [i.e., the Mohr-Coulomb failure criterion is taken to be the fit regression straight line passing through zero in the (σ_n, τ) diagram].

2.1.3. Small-scale shear device

This ssSD (Figure 4) was developed to determine the mechanical resistance of geosynthetic-geosynthetic interfaces on a small scale (i.e., for surface dimensions on the order of 10 cm x 10 cm) and at relatively low normal stress (i.e., up to 10 kPa, but fixed at 5 kPa in the present study). This surface area is appropriate for analysing the interface between geomembranes and nonwoven needle-punched geotextiles that are continuous with highly homogeneous surfaces.

In this device, a 20 cm x 15 cm geomembrane is fixed to a supporting structure with a high-friction surface (P80 abrasive sheet) to avoid any displacement of the geomembrane. Next, a 10 cm x 10 cm geotextile is subjected to the requisite normal stress by using a non-deformable metallic plate. To avoid any relative displacement between the geotextile and the metallic plate, the latter is covered with a high-friction P80 abrasive sheet. In any case, for each test, the condition of zero relative displacement between the geomembrane and its support and between the geotextile and the metallic plate must be verified. The maximal displacement of the geotextile that slides onto the geomembrane is 25 mm, thus corresponding to 25 % of the length of the specimen. Whatever the way of applying shear stress, the tangential displacement of the metallic plate is monitored during the whole test by a Mitutoyo absolute Digimatic Indicator (measurement accuracy of 0.003 mm).

There are two ways to impose shear with the ssSD (Figure 4):

- Shear stress may be imposed at the interface incrementally. To implement this procedure, masses are added to a supporting structure at each step time so that the interface shear stress increases incrementally via a cable connecting the supporting structure to the metallic plate. This loading method is similar to that used for the IP test if the plane inclination is increased incrementally.
- A constant velocity parallel to the interface may be imposed at the metallic plate by using an electric stepper motor, from a Wykeham Farrance shear machine, with a speed range from 0.001 to 10 mm/min; the minimum speed being a mean value of the stepped motion. This loading method is completely equivalent to that used by the large-scale SB device.

This ssSD offers several advantages compared with the large-scale IP device and the large-scale SB device:

- For loading by increasing the shear stress incrementally, the small-scale shear device allows more tests to be made, and in an easier manner, especially compared with the large-scale IP device, which requires the handling of 500 kg of sand for each test.
- For loading by increasing the tangential displacement, the small-scale shear device can impose a very small velocity (0.001 to 10 mm/min), whereas the minimum velocity for the large-scale SB is only 0.1 mm/min. Moreover, the ssSD is very accurate and precise for producing very low normal stress (e.g., 5 kPa), whereas the large-scale SB is not as precise for low normal stress because its hydraulic jack is designed for high normal stress.

2.2. Geosynthetics tested in this study

Four types of geomembranes were tested in this study:

- a high-density polyethylene geomembrane (HDPE GMB);
- an ethylene-propylene-diene terpolymer geomembrane (EPDM GMB);
- a polypropylene geomembrane (PP GMB);
- a polyvinyl chloride geomembrane (PVC GMB).

All geomembranes tested were smooth (i.e., no textured surface) and had homogeneous mass (i.e., non-armed, non-structured). The geotextile tested was a non-woven needle-punched geotextile, designed as GTX_{nw}. Table 1 summarises the main physical properties of the geosynthetics tested. The thickness and mass per unit area of the geomembranes were measured according to the standard EN 1849-2, and the thickness (at 2 kPa) and mass per unit area of the geotextiles were measured according to the standards EN ISO 9863-1 and EN ISO 9864, respectively. This study tested the interfaces between the fourth geomembranes and the GTX_{nw} geotextile. The large-scale SB and IP

tests, that required an overlying soil on the geomembrane-geotextile interface, used the standardised sand as per the standards EN ISO 12957-1 and-2.

2.3. Experimental Program

The introduction emphasises that temperature can influence the shear resistance of interfaces between geosynthetics. The standards EN ISO 12957-1 and EN ISO 12957-2 require that the geosynthetics product be conditioned and the test done at 20 ± 2 °C. The large-scale SB was located in the geomechanical lab in Irstea, Aix-en-Provence (Figure 1), where the temperature was regulated within the recommended temperature range. Likewise, the ssSD was located in the geosynthetics lab in Irstea, Aix-en-Provence, where the temperature was also regulated. The IP device is a very large apparatus that was housed in a high-ceiling experimental hall where the temperature was not regulated. For tests involving the IP device, the product was well conditioned at the required temperature and the tests were done at a measured (unregulated) temperature of 21 ± 3 °C (i.e., at a slightly greater temperature than that for the tests involving the large-scale SB and ssSD).

2.3.1. Tests of four interfaces

Large-scale IP tests were done with the four geomembrane-geotextile interfaces following EN ISO 12957-2 and with a normal stress of 5 kPa. The same device was used for other tests in which the plane inclination was increased, step by step, in 1° increments per hour.

2.3.2. Tests of PP GMB -GTX_{nw} interface

To better understand the behaviour of the PP-GTX_{nw} interface, tests were done with the large-scale SB following EN ISO 12957-1 and with another procedure in which a speed of 0.1 mm/min was imposed instead of the standard speed of 1 mm/min. Recall that, in this test, the confining normal stress ranged from 50 to 150 kPa, so the results cannot be directly compared with those from the IP test.

Finally, an exhaustive suite of tests was done with the ssSD in which a normal stress of 5 kPa was imposed for all tests and shear was imposed either (i) by increasing the shear stress step by step at rates varying incrementally from 0.1 kPa per minute (first series of three tests) to 0.1 kPa per 30 min (second series of three tests) [note that increasing the shear stress by 0.1 kPa on an interface confined by a normal stress of 5 kPa correspond to an increase of about 1° (arctan 0.1/5 ≈ 1.1°) in terms of interface friction angle], or (ii) by increasing the tangential speed at a constant rate (from 0.001 to 5 mm/min, depending on the test). For incremental loading shear tests, the shear rate of 0.1 kPa per 30 min (i.e., approximately equivalent to 1° in terms of friction angle per 30 min) applied in the ssSD tests was slightly higher than the shear rate of 1° of plane inclination per hour (i.e., approximately equivalent to 1° in terms of friction angle per hour) applied in large-scale IP tests. This rate allowed each test to be done in one day.

3. Results

3.1. Inclined-plane tests

Figure 5a shows the results of IP tests on the four geomembrane-geotextile interfaces; these tests were done following the procedure given by EN ISO 12957-2. As is often reported in the literature (see, for example, Briançon et al., 2011), the HDPE GMB-GTX$_{nw}$ interface exhibits a sudden sliding behaviour whereas the other interfaces, which involve more flexible geomembranes, exhibit a gradual sliding behaviour. Table 2 lists the interface angles obtained at β_{is} (at δ_{IP} = 1 mm, as done by Pitanga et al., 2009) and the calculated standardised interface friction angle φ_{50}, at β_{50} (at δ_{IP} = 50 mm). These results were obtained by following the methodology given in EN ISO 12957-2.

For the three interfaces that undergo gradual sliding, the upper box begins to slide at the plane inclination β_{is} equal to about 10°, which is much less than the plane inclination β_{50}, that is used for calculating the standardised interface friction angle. The results given in Table 2 show that the interface angles at β_{is} are much smaller than those obtained by using the current standard, except for the HDPE GMB-GTX$_{nw}$ interface.

When the upper box reaches 1 mm of tangential displacement (at β_{is}), the interface may remain stable (i.e., the interface described in the introduction has not yet reached the "peak displacement"). Thus, the interface friction angle calculated from β_{is} may be too conservative. The interface sliding speeds for all tests displayed in Figure 5a were assessed and are displayed in Figure 5b to allow for a more in-depth analysis of the onset of sliding. For the HDPE GMB-GTX$_{nw}$ interface, the upper box accelerates significantly at $\beta_{is}(\delta_{IP} = 1\ mm) = 10.6°$. This value is close to the plane inclination $\beta(\delta_{IP} = 50$ mm) = 11.1°, used in the standard EN ISO 12957-2 to calculate the (standardised) friction angle. Conversely, at $\beta_{is}(\delta_{IP} = 1$ mm), the gradual-sliding interfaces exhibit very small sliding speeds (on the order of 0.01 mm/min).

To investigate in more detail the onset of instability of the gradual-sliding interfaces, further inclined plane tests were done following a testing procedure that differs from that of EN ISO 12957-2. These tests involved incrementing the plane inclination by 1° each hour while measuring the displacement of the upper box during the entire test. Contrary to the standardised testing procedure where the plane inclination is increased at constant rate of 3°/min, this testing procedure more accurately determines (by virtue of the 1° increments in plane inclination) the speed at the tested interface over 1 hour. Figure 6 shows the resulting displacement of the upper box as a function of plane inclination. At first sight, gradual sliding at the tested interfaces is not clearly observed, unlike the case shown in Figure 5a. Also, the plane is much less inclined for $\delta_{IP} = 50$ mm than is the case for the displacement curves shown in Figure 5a, except for the HDPE GMB-GTX$_{nw}$, which underwent sudden sliding following the standardised testing procedure. To accurately determine the plane inclination at which sliding begins at the interface, the sliding at each interface was analysed separately.

For the HDPE GMB-GTX$_{nw}$ interface (see results in Figure 7), the upper box was stable up to a plane inclination of 12°. However, 40 s after the change of plane inclination to 13°, the upper box suddenly began to slide. The interface friction angle determined from the plane inclination of 12.5° gave a larger friction angle than that determined from the standardised testing procedure. Considering that

this interface underwent a small displacement before failure (i.e., δ_{IP} = 2.2 mm at the end of the stage β = 12° in the case of the test carried out following the incremental testing procedure) it may be suggested that the standardised testing procedure, where the plane inclination is increased at a constant rate, contributes to a more rapid onset of interface failure. Additional tests should be carried out to confirm this observation.

For the EPDM GMB-GTX$_{nw}$ interface (see results in Figure 8), the upper box of the IP tests remains static up to a plane inclination of 18°. Figure 8 plots as a function of time both the displacement and the sliding speed for the plane inclination β = 19°. For the first ten minutes, the displacement of the upper box slowly increases at a speed of 0.1 to 0.4 mm/min. After 10 min, the speed at the interface increases more rapidly. This relatively surprising sliding behaviour is obtained for a constant imposed τ_{IP} /σ_{IP}. From β = 18.5°, a new friction angle of 24.7° ± 0.7° is obtained (Table 2), which is to be compared with the friction angle of 31.1° ±0.2° obtained by using the procedure of EN ISO 12957-2.

For the PVC GMB-GTX$_{nw}$ interface (see results displayed in Figure 9), the upper box remains static up to a plane inclination of 14°. However, for β > 14°, the upper box slides, at a constant speed of 0.4 mm/min for β = 15° and of about 0.5 mm/min for β = 16°. For β = 14.5°, a new friction angle of 19.3° ± 0.7° is obtained (see Table 2), which is to be compared with the friction angle of 36.8° ± 0.2° obtained by using the procedure EN ISO 12957-2.

The PP GMB-GTX$_{nw}$ interface (see results displayed in Figure 10a) remains static up to a plane inclination of 9°. Then, for β = 10°, the upper box slides at a very low and constant speed of about 0.002 mm/min. As the plane inclination increases 1° per hour, the sliding speed progressively increases up to 4.6 mm/min for β = 21° (Figure 10b). Compared with the previous two gradual-sliding interfaces, the very low sliding speed (about 0.002 mm/min) prevents us from clearly determining the plane inclination at which interface failure occurs: should the plane inclination β = 9.5° has to be considered to determine the interface friction angle? At this very low sliding speed, the hourly incrementation of plane inclination prevents us from answering this question. For such interface, a

specific study using a large-scale shear box and a small-scale shear box was done to determine the sliding behaviour as a function of shear stress.

3.2. Large-Scale Shear Box Tests

For the PP GMB-GTX$_{nw}$ interface, the shear box can be adapted to study how sliding speed at the interface depends on shear stress, because a constant speed can be imposed at the interface while the shear stress is recorded. So a large-scale shear box device was used to test this interface following the standard EN ISO 12957-1 and at the standardised speed of 1 mm/min. Another series of tests were performed with the standardised speed changed to 0.1 mm/min. The results of all tests are given in Figure 11 and Table 3. The experimental results show that the lowest speed leads to lower interface shear stress by about 20 %, observed in the residual part of the shear curve (i.e. shear stress evaluated at δ = 20 mm in Table 3). To use these curves to determine the friction angles of the PP GMB-GTX$_{nw}$ interface (see values in Figure 11b), both the peak shear stress and the minimal shear stress obtained after the peak were considered (see analysis method in §2.1.2.). Friction angles were determined from the best linear fit to the data in the planes (σ_n, τ_{SBpeak}) and (σ_n, $\tau_{SBp\text{-}peak}$). With the large-scale shear box, the decrease in speed from 1 to 0.1 mm/min leads to a decrease of 1.1° in the post-peak interface friction angle.

These friction angles are obtained for a normal stress range from 50 to 150 kPa, so they cannot be compared with the friction angles obtained from the IP tests where the imposed normal stress was 5 kPa. Also, our large-scale SB device does not allow us to use a speed below 0.1 mm/min. Thus, the dependence of sliding speed at the interface on the shear stress cannot be studied for very low shear speeds (in the range of 0.001 to 0.1 mm/min, which are measured in the IP tests; see §3.1). Thus, at this stage, it is not possible to conclude whether it is better to determine the friction angle for gradual sliding at the interface by imposing shear stress and measuring displacement or by imposing displacement at a constant speed and measuring shear stress.

3.3. Small-Scale Shear Device tests

3.3.1. Comparison of two ways of applying shear

To investigate in detail how sliding at the interface is related to the shear stress for the PP GMB-GTX_{nw} interface, the ssSD described in §2.1.3 was used. To make a reliable comparison, all shear tests were done at the normal stress of 5 kPa. A complete description of the tests is provided in §2.3.2.

Interface shear tests were done by increasing the shear stress incrementally at three interfaces at a rate of 0.1 kPa every minute and at a rate of 0.1 kPa every 30 min. The results (see Figure 12) give rise to two remarks: as already observed for the large-scale IP tests, the maximal displacement of 25 mm is reached at a lower shear stress, when the shear rate was lower (ie. 0.1 kPa per each 30 min). In addition, the shear curves vary, whereas the geomembrane and geotextile that were tested were homogeneous. In our experience, such variability can occur also with IP tests, even for a test surface of 1 m x 1 m.

Another series of interface shear tests were done by imposing a constant tangential velocity ranging from 0.001 to 5 mm/min, depending on the test. The results are shown in Figure 13. The interface was tested three times, with virgin specimens of geomembrane and geotextile, at each speed (except for 0.001 mm/min). As found when using the large-scale SB test but for a limited speed range, the shear rate of the PP GMB-GTX_{nw} interface strongly depends on the speed imposed. In addition, the variability in the test results seems to diminish compared with tests done with an increasing shear stress. The maximal gap between the measured shear stress is 0.3 kPa, whereas it was 0.8 kPa in the previous series of tests.

The main goal of these two series of tests was to determine which testing method (i.e., increasing shear stress incrementally or imposing a constant velocity tangential to the interface) is more appropriate to reliably determine the interface friction angle. Toward this end, the results of the two series of tests are regrouped in Figure 14, where the speed at the interface (measured in the first series of tests and imposed in the second series of tests) is given as a function of shear stress

(imposed in the first series of tests and measured in the second series of tests). For the first series of tests, only the three tests for which the shear increased at 0.1 kPa every 30 min were considered, because these tests produced more reliable results for the sliding speed of sliding (i.e., the time intervals for the three tests for which the shear increased at 0.1 kPa per minute were too short to properly assess the sliding speed at each shear stress). For the tests at constant displacement rate, the shear stress was assessed from the mean of the three tests at each constant displacement rate (see results in Figure 13) at the same level displacement δ_{ssSD} = 5 mm (this value was chosen based on the tests done at 0.01 mm/min). The results in Figure 14 show that, for the tests where the shear stress increases incrementally, the onset of sliding at the interface seems to begin at a very low speed of sliding (i.e., 0.001 mm/min). For the three tests for which the shear increased incrementally, the sliding speed was sometimes found to be less than 0.001 mm/min. These very low sliding speeds suggest that the displacement measured at each step corresponds to the creep phenomenon. Tests with long time intervals between each step should be done to confirm this hypothesis. In the large-scale IP test, such profile of sliding speed as a function of shear stress [i.e., plane inclination following equation (1)] was observed (see §3.1. and Figures 10a and 10b). For the series of tests with constant tangential velocity at the interface, the imposed speed of 0.001 mm/min leads to a measured shear stress of about 1.75 kPa, which is about the same value that occurs at the onset of sliding at the interface (at the same speed of 0.001 mm/min) in the first series of tests. Thus, from the results of the interface shear test with constant tangential velocity at the interface of 0.001 mm/min, the measured shear stress is reliable for determining the interface friction angle. Moreover, based again on Figure 14, the series of tests in which the shear stress increases incrementally does not allow us to determine with certainty the onset of sliding at the interface, because the time interval between stress increments is too short (the same remark applies to the IP test discussed in §3.1.). Thus, another test using the IP device but in which the plane inclination was increased by 1° every 24 hours is discussed in §3.3.3.

3.3.2. Effect of Successive Slides

As is often observed (see introduction), successive episodes of sliding at an interface can modify the interface friction angle, which can be a major problem for ensuring the long-term stability of GLSs in geostructures. This point was investigated in a detailed study of the PP GMB-GTX$_{nw}$ interface.

The ssSD was used to test successive episodes of sliding at an interface by using the shear method implemented both by incrementally increasing the shear stress and by imposing a constant tangential velocity. More specifically, a series of four successive shear tests were done in which the shear stress was incrementally increased at the interface of a virgin geomembrane specimen and a virgin geotextile specimen (see results in Figure 15a), and another series of four successive shear tests were done by imposing a constant tangential velocity at the interface of another virgin geomembrane specimen and another virgin geotextile specimen (see results in Figure 15b). For both series of tests, the successive episodes of sliding lead to a clear decrease of the interface shear stress. However, these two series of tests alone do not allow us to determine whether this decrease in shear stress is due to modifications of the friction characteristics of the geomembrane, of the geotextile, or both.

Another series of successive shear tests were made, this time by imposing a constant tangential velocity at the interface formed by a single geomembrane specimen and four different geotextile specimens, and vice versa. In this way, the single specimen in each series of tests is subjected to successive episodes of sliding whereas the four different specimens are not. The results of these two series of tests are displayed in Figures 16a and 16b, respectively. For the first series of tests (where the geomembrane specimen is subjected to the successive episodes of sliding), Figure 16a reveals a decrease of the interface shear stress following the successive episodes of sliding. Conversely, for the second series of tests, where the geotextile specimen is subjected to successive episodes of sliding, the friction characteristics do not change beyond the normal noise expected in these experimental results.

These series of tests lead to the conclusion that the friction characteristics of the PP GMB-GTX_{nw} interface are sensitive to sliding and, in particular, that they decrease after successive episodes of sliding.

Note that the variability in the shear curves of Figure 16b, which was already highlighted in Figure 12, suggests that, even if the geomembrane appears thoroughly homogeneous, the friction characteristics of the surface can be heterogeneous on the scale of a 10 cm x 10 cm specimen.

3.3.3. Discussion: how best to determine the interface friction angle for the GMB-GTX_{nw} interface

The series of tests with the large-scale IP device shows that the GMB–GTX_{nw} interface that exhibits gradual sliding clearly leads to an overestimate of the friction angle when following the testing procedure of EN ISO 12957-2. A modified testing procedure in which the plane inclination is increased in 1° increments leads to a more reliable interface friction angle. However, the interface failure for the PP GMB-GTX_{nw} interface is difficult to determine accurately, probably because the time interval between increments in plane inclination was too short [the time interval of 1 hour (for each increment of 1° of plane inclination) was too short to clearly distinguish the interface sliding (i.e. failure reached) versus the creep phenomenon].

The series of tests using the ssSD shows that imposing shear both by (i) increasing the shear stress incrementally at the interface and (ii) imposing a constant tangential velocity at the interface leads to relatively similar results. However, method (i) makes it difficult to accurately determine the onset of sliding at the interface because of the very small initial sliding speed (on the order of 0.001 mm/min). To overcome this problem, longer time intervals between increments should be used. Moreover, determining the safest value of the interface shear resistance by imposing a constant tangential velocity requires the use of a very low speed (on the order of 0.001 mm/min). Finally, a last series of tests with the ssSD showed that successive episodes of sliding lead to a significant reduction in the magnitude of the friction at the PP GMB-GTX_{nw} interface. This decrease in the magnitude of the friction was shown to be due to modifications of the geomembrane surface and was not affected by

the nonwoven needle-punched geotextile. A better understanding of the physical modifications occurring at the geomembrane surface will be the goal of a future study.

Finally, the PP GMB-GTX$_{nw}$ interface was subjected to two large-scale IP tests: a first test in which shear was imposed incrementally by incrementing the plane inclination by 1° per hour (see results in Figure 10), and a second test, with same specimen as in the first test, in which shear was imposed incrementally by incrementing the plane inclination by 1° per day (24 hours). The results displayed in Figures 17a and 17b show that the interface remained stable up to an inclination of 9°. However, at a plane inclination of 10°, the interface remained stable only for the first 7 hours, after which began a continuous sliding at the interface, reaching a sliding speed of 0.02 mm/min. Thus, compared with results in Figures 10a and 10b where the interface failure could not be accurately determined, the present test clearly indicates that a plane inclination of 10° causes the interface to fail. Inserting a plane inclination of 9.5° into equation (3) then gives the PP GMB-GTX$_{nw}$ interface friction angle (see Table 2). Finally, the result of 12.9 ± 0.7° can be considered as the safest friction angle for the PP GMB-GTX$_{nw}$ interface when designing long-term geosynthetic lining systems.

4. Conclusions

This study highlights the limits of the two current standards EN ISO 12957-1 and -2 that are used to determine the interface friction angle for geosynthetics, experiments on the interface between smooth geomembranes and nonwoven needle-punched geotextiles were performed to better understand the complex behaviour of such interfaces as a function of shear and interface sliding velocity.

The results lead to the following main conclusions:

- Large-scale IP tests on the four EPDM, PP, PVC and HDPE GMB-GTX$_{nw}$ interfaces underlined the various complex behaviours of such various interfaces with regards to sliding speed versus increasing shear rate. For the HDPE GMB-GTX$_{nw}$ interface that underwent sudden sliding following the standardised IP test, the incremental testing procedure may give a

greater friction angle. Conversely, for the other EPDM, PP, PVC GMB-GTX_{nw} interfaces that exhibited gradual sliding following the standardised testing IP test, the incremental testing procedure modified the gradual sliding behaviour and led to lower friction angles. Further research is needed to completely assess how the standardised incremental testing procedures of the IP test affect the various types of GMB-GTX interfaces. Such research may lead to modifications of the current standard EN ISO 12957-2 for the IP test.

- Large-scale IP tests on the EPDM, the PP, and the PVC GMB-GTX_{nw} interfaces show that the speed of sliding at the interface is strongly affected by the interface friction shear stress, which increases with interface sliding rate for these three tested interfaces. In particular, for the PP GMB-GTX_{nw} interface and using the incremental shear-loading mode, the initial interface sliding speed was very low; on the order of 0.001 mm/min. This result explains the gradual sliding behaviour of such GMB -GTX_{nw} interfaces when subjected to the IP test following the current standard EN ISO 12957-2. In fact, during such a test, sliding at the interface can begin at β_{is} at a very low speed, and, because the shear stress increases with plane inclination, the interface sliding speed increases continuously. In conclusion, for the tested EPDM, the PP, and the PVC GMB-GTX_{nw} interfaces, the testing method that determines the interface friction angle based on a 50 mm tangential displacement at the interface leads to overestimates of the interface friction angle.
- To reliably determine the tested EPDM, the PP, and the PVC GMB-GTX_{nw} interface friction angle by using the IP test, the results show that the IP test should be done by incrementally increasing the plane inclination. To clearly determine which plane inclination leads to unstable sliding, the time interval between increments should be as long as possible. Further research is needed to determine the best time interval to use between increments to avoid excessively long tests. This conclusion applies to the EPDM, the PP, and the PVC GMB-GTX_{nw} interfaces tested in the present study. Changing the nature or type of geomembrane (for

example, HDPE GMB as seen in this study) should imply a specific study (i.e., a comparison between the standardised and incremental testing procedures of the IP test).

- The friction properties dependency with sliding speed was evidenced by direct shear tests at constant speed. Other authors (as Pavanello et al., 2018a; Wartman et al., 2003; Yegian and Kadakal, 1998) observed an increase of the GMB-GTX (smooth HDPE GMB – GTX_{nw} in the above studies) interface friction angle with sliding speed but in the case of dynamic tests (i.e., that determine dynamic friction angle). This study shows that to reliably determine the PP GMB-GTX_{nw} interface "static" friction angle by using the SB test, it should follow the current standard EN ISO 12957-1 but the shear test should be done at very low sliding speeds (i.e., 0.001 mm/min). Further studies are necessary to determine how the rate of displacement affects the interface shear resistance for all possible geomembrane/geotextile interfaces.
- For the PP GMB-GTX_{nw} interface, successive episodes of sliding lead to a decrease in interface shear resistance, which could be attributed to the modification of the friction characteristics of the PP GMB surface. To design a stable, long-term critical structure that involves GLSs that include such PP GMB-GTX_{nw} interfaces (and thereby ensure its sustainability), successive tests should be done to determine the safest friction angle. Once again, further studies are required to investigate if or how successive episodes of sliding can modify the friction properties of other geomembrane/geotextile interfaces.

Finally, the insufficiencies of the current standards EN ISO 12957-1 and -2 are strongly evinced and various possible ways to improve them are given.

Acknowledgments

Some results of this study were obtained within the framework of the Interreg ALCOTRA Resba project, with Feder ERDF (European Regional Development Fund) financial support. The authors are

grateful to Julien Aubriet, Clément Bruneau, Maxime Feced, and Keinny François for their help in carrying out some of the tests in this study.

Notations

A	(m^2)	contact area of a tested interface
fr(β)	(N)	force required to hold back the empty upper box at β in the inclined plane test
fr(β_{50})	(N)	force required to hold back the empty upper box at β_{50} in the inclined plane test
t	(s)	time
v	($m.s^{-1}$)	rate of displacement
β	(°)	inclination of the plane in the inclined plane test
β_{is}	(°)	inclination of the plane at initial sliding in the inclined plane test
β_{50}	(°)	standardised plane inclination in the inclined plane test to determine φ_{50}
δ_{IP}	(mm)	tangential displacement in the inclined plane test
δ_{50}	(mm)	tangential displacement at β_{50} in the inclined plane test
δ_{SB}	(mm)	tangential displacement in the shear box test
δ_{ssSD}	(mm)	tangential displacement in the small-scale shear device test
φ_{50}	(°)	standardised friction angle in the inclined plane test
φ_{SBpeak}	(°)	peak friction angle in the shear box test
$\varphi_{SBp\text{-}peak}$	(°)	post-peak friction angle in the shear box test
σ_n	(kPa)	normal stress
σ_0	(kPa)	initial normal stress at β = 0° in the inclined plane test
σ_{IP}	(kPa)	normal stress in the inclined plane test
τ_{IP}	(kPa)	shear stress in the inclined plane test
τ_{SB}	(kPa)	shear stress in the shear box test
τ_{SBpeak}	(kPa)	maximum shear stress of the curve (δ_{SB}, τ_{SB})
$\tau_{SBp\text{-}peak}$	(kPa)	plateau of the curve (δ_{SB}, τ_{SB})
τ_{ssSD}	(kPa)	shear stress in the small-scale shear device test

References

Bacas, B. M., Cañizal, J., Konietzky, H., 2015a. Frictional behaviour of three critical geosynthetic interfaces. Geosynth. Int. 22 (5), 355–365.

Bacas, B.M., Cañizal, J., Konietzky, H., 2015b. Shear strength behavior of geotextile/geomembrane interfaces. J. Rock Mech. Geotechnical Eng. 7 (6), 638-345.

Briançon, L., Girard, H., Gourc, J.-P., 2011. A new procedure for measuring geosynthetic friction with an inclined plane. Geotext. Geomembranes 29 (5), 472-482.

Briançon, L., Girard, H., Poulin, D., 2002. Slope stability of lining systems: experimental modeling of friction at geosynthetic interfaces. Geotext. Geomembranes 20 (3), 147-172.

Carbone, L., Gourc, J.P., Carrubba, P., Pavanello, P., Moraci, N., 2015. Dry friction behaviour of a geosynthetic interface using inclined plane and shaking table tests. Geotext. Geomembranes 43 (4), 293-306.

De, A., Zimmie, T.F., 1998. Estimation of dynamic interfacial properties of geosynthetics. Geosynth. Int. 5 (1–2), 17–39.

EN 1849-2, 2010. Flexible sheets for waterproofing - Determination of thickness and mass per unit area - Part 2 : plastic and rubber sheets. European Committee for Standardization.

EN ISO 9863-1, 2016. Geosynthetics - Determination of thickness at specified pressures - Part 1 : single layers. International Committee for Standardization.

EN ISO 9864, 2005. Geosynthetics - Test method for the determination of mass per unit area of geotextiles and geotextile-related products. International Committee for Standardization.

EN ISO 12957-1, 2018. Geosynthetic - Determination of Friction Characteristics, Part 1: Direct Shear Test. International Committee for Standardization.

EN ISO 12957-2, 2005. Geosynthetic - Determination of Friction Characteristics, Part 2: Inclined Plane Test. International Committee for Standardization.

Ferreira, F.B., Vieira, C.S., Lopes, M.L., 2015. Direct shear behaviour of residual soil–geosynthetic interfaces – influence of soil moisture content, soil density and geosynthetic type. Geosynth. Int. 22 (3), 257-272.

Fowmes, G.J., Dixon, N., Jones, D.R.V., 2008. Validation of a numerical modelling technique for multi-layered geosynthetic landfill lining systems. Geotext. Geomembranes 26 (2), 109-121.

Fox, P. J., Ross, J. D., Sura, J. M. & Thiel, R. S., 2011. Geomembrane damage due to static and cyclic shearing over compacted gravelly sand. Geosynth. Int. 18 (5), 272–279.

Fox, P. J., Thielmann, S. S., 2014. Interface Shear Damage to a HDPE Geomembrane. II: Gravel Drainage Layer. J. Geotech. Geoenviron. Eng. 140 (8) 12p.

Fox, P. J., Thielmann, S. S., Stern, A. N., Athanassopoulos, C., 2014. Interface shear damage to a HDPE geomembrane. I: Gravelly compacted clay liner. J. Geotech. Geoenviron. Eng. 140 (8), 14p.

Frost, J. D., Karademir, T., 2016. Shear-induced changes in smooth geomembrane surface topography at different ambient temperatures. Geosynth. Int. 23 (2), 113–128.

Frost, J.D., Lee, S.W., 2001. Microscale Study of Geomembrane- Geotextile Interactions. Geosynth. Int. 8 (6), 577-597.

Giroud, J.P., Beech, J.F., 1989. Stability of soil layers on geosynthetic lining system. San Diego, USA Proc. Geosynth. Conf. 35-46.

Giroud, J.P., Williams, N.D., Pelte, T., Beech, J.F., 1995. Stability of Geosynthetic-Soil Layered Systems on Slopes. Geosynth. Int. 2 (6), 1115-1148.

Hanson, J. L., Chrysovergis, T. S., Yesiller, N., Manheim, D. C., 2015. Temperature and moisture effects on GCL and textured geomembrane interface shear strength. Geosynth. Int. 22 (1), 110–124.

Hebeler, G.L., Frost, J.D., Myers, A.T., 2005. Quantifying hook and loop interaction in textured geomembrane–geotextile systems. Geotext. Geomembranes 23 (1), 77–105.

Hillman, R.P., Stark, T.D., 2001. Shear Strength Characteristics of PVC Geomembrane-Geosynthetic Interfaces, Geosynth. Int. 8 (2), 135-162.

Kim, D., Frost, J.D., 2011. Effect of geotextile constraint on geotextile/geomembrane interface shear behavior. Geosynth. Int. 18 (3), 104–123.

Kim, J., Riemer, M., Bray, J.D., 2005. Dynamic properties of geosynthetic interfaces. Geotech. Test J. 28 (3), 1–9.

Koerner, R.M., Hwu, B.-L., 1991. Stability and tension considerations regarding cover soils on geomembrane lined slopes. Geotext. Geomembranes 10 (4), 335-355.

Koerner, R.M., Soong, T.Y. ,2000. Leachate in landfills: the stability issues. Geotext. Geomembranes 18 (5), 293-309

Koutsourais, M.M., Sprague, C.J., Pucetas, R.C., 1991. Interfacial friction study of cap and liner components for landfill design. Geotext. Geomembranes 10 (5-6), 531-548.

Lopes, M.L., Ferreira, F.B., Vieira, C.S., 2014. Soil–geosynthetic inclined plane shear behavior: influence of soil moisture content and geosynthetic type. Int. J. of Geotech. Eng. 8 (3), 335-342.

Martin, J.P., Koerner, R.M., 1985. Geotechnical Design Considerations for Geomembrane Lined Slopes: Slope Stability. Geotext. Geomembranes 2 (4), 299-321

Palmeira, E.M., Lima, Jr. N.R., Mello, L.G.R., 2002. Interaction between soils and geosynthetic layers in large-scale ramp tests. Geosynth. Int. 9 (2), 149-187.

Pavanello, P., Carrubba, P., Moraci, N., 2018a. Dynamic friction and the seismic performance of geosynthetic interfaces. Geotext. Geomembranes 46 (6), 715-725.

Pavanello, P., Carrubba, P., Moraci, N., 2018b. The determination of interface friction by means of vibrating table tests. Geotext. Geomembranes 46 (6), 830-835.

Pitanga, H.N., Gourc, J-.P., Vilar, O.M., 2009. Interface shear strength of geosynthetics: evaluation and analysis of inclined plane test. Geotext. Geomembranes 27 (6), 435- 446.

Reyes-Ramirez, R., Gourc, J-.P., 2003. Use of the inclined plane test in measuring geosynthetic interface friction relationship. Geosynth. Int. 10 (5), 165-175.

Stark, T. D., Choi, H., 2004. Peak versus residual interface strengths for landfill liner and cover design. Geosynth. Int. 11 (6), 491–498.

Stark, T. D., Newman, E. J., Aust, R. L., 2008. Back-analysis of a PVC geomembrane-lined pond failure. Geosynth. Int. 15 (4), 258–268.

Stark, T. D., Poeppel, A. R., 1994. Landfill liner interface strengths from torsional ring shear tests. J. Geotech. Eng. 120 (3), 597–615.

Stark, T.D., Williamson, T.A., Eid, H.T., 1996. HDPE Geomembrane/Geotextile Interface Shear Strength, J. Geotech. Eng. 122 (3), 197-203.

Stoltz, G., Auray, G., 2014. Comparison of various testing methods for soil-geogrid friction parameters estimation to stabilise a thin soil layer on slopes. 10th International Conference on Geosynthetics, Berlin, Germany.

Stoltz, G., Gallo, R., Poulain, D., Touze-Foltz, N., 2012. Improvement of the inclined plane device to assess the friction properties at geosynthetics interfaces. Eurogeo 5 ,Valencia, Spain, 5 p.

Stoltz, G., Hérault, A., 2014. Assessing interface friction angles of geosynthetics by comparing two loading methods. 10th International Conference on Geosynthetics, Berlin, Germany.

Stoltz, G., Vidal, N., 2013. Alteration of friction characteristics of geosynthetics interfaces following successive slidings. Int. Symp. on Design and Practice of Geosynthetic-Reinforced Soil Structures, Bologna, Italy, 6p.

Tano, B.F.G., Dias, D., Fowmes, G.J., Olivier, F., Stoltz, G., Touze-Foltz, N., 2016. Numerical modeling of the nonlinear mechanical behaviour of multilayer geosynthetic system for piggy-back landfill expansion. Geotext. Geomembranes 44 (6), 782-798.

Tano, B. F. G., Dias, D., Stoltz, G., Touze-Foltz, N., Olivier, F., 2017a. Numerical modelling to identify key factors controlling interface behaviour of geosynthetic lining systems. Geosynth. Int. 24 (2), 167–183.

Tano, B. F. G., Stoltz, G., Touze-Foltz, N, Dias, D., Olivier, F., 2017b. A numerical modelling technique for geosynthetics validated on a cavity model test. Geotext. Geomembranes 45 (4), 339-349.

Thiel, R.S., 1998. Design methodology for a gas pressure relief layer below a geomembrane landfill cover to improve slope stability. Geosynth. Int. 5 (6), 589-617

Vieira, C.S., Lopes, M.L., Caldeira, L.M., 2013. Sand-geotextile interface characterisation through monotonic and cyclic direct shear tests. Geosynth. Int. 20 (1), 26-38.

Wartman, J., Bray, J.D., Seed, R.B., 2003. Inclined plane studies of the Newmark sliding block procedure. J. Geotech. Geoenviron. Eng. 129 (8), 673–684.

Wasti, Y., Özdüzgün, Z.B., 2001. Geomembrane–geotextile interface shear properties a s determined by inclined board and direct shear box tests. Geotext. Geomembranes 19 (1), 45–57.

Yegian, M.K., Kadakal, U., 1998. Geosynthetic interface behavior under dynamic loading. Geosynth. Int. 5 (1–2), 1–16.

Yegian, M.K., Lahlaf, A.M., 1992. Dynamic interface shear strength properties of geomembranes and geotextiles. J. Geotech. Eng. 118 (5), 760–779.

Yesiller, N., Manheim, D., Hanson, J., Chrysovergis, T., 2016. Temperature-Dependent Variation in Surface Characteristics Of A Textured Geomembrane Due to Interface Shear Testing Against A GCL. Geo-Americas 2016, Miami Beach, USA, 3rd Pan-American Conference on Geosynthetics.

Zettler, T.E., Frost, J.D., DeJong, J.T., 2000, Shear-Induced Changes in Smooth HDPE Geomembrane Surface Topography, Geosynth. Int. 7 (3), 243-267.

Figure 1. Large-scale inclined plane (left) and large-scale shear box (right) in Irstea Aix-en-Provence.

Figure 2. Schematic principle of (a) the IP test and (b) the SB test.

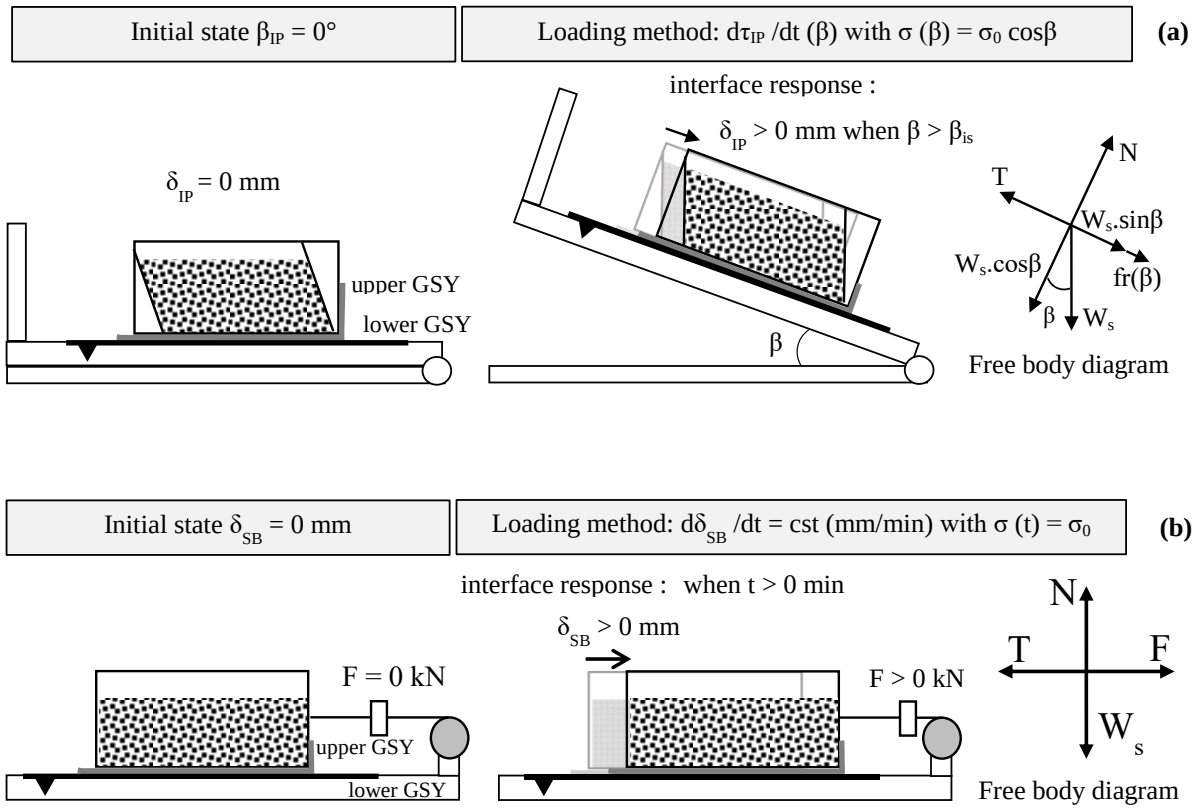

Figure 3. Two typical interface sliding behaviours from the IP test and two typical interface shear behaviours from the SB test.

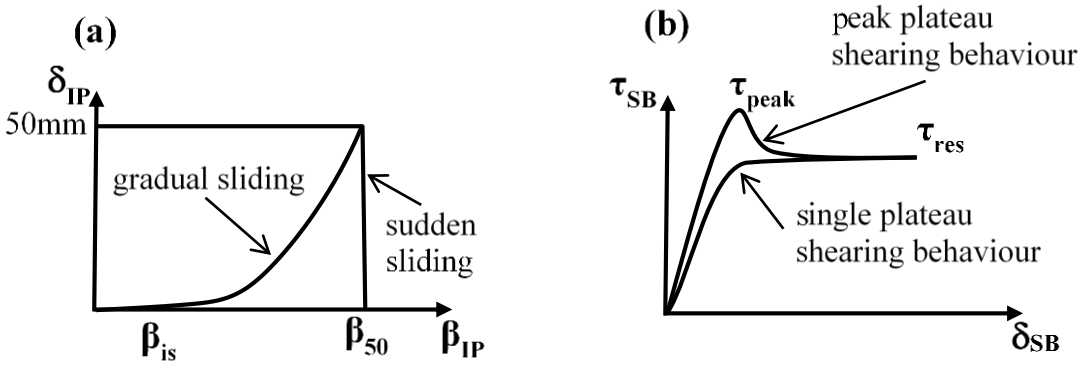

Figure 4. Schematic principle of small-scale shear device.

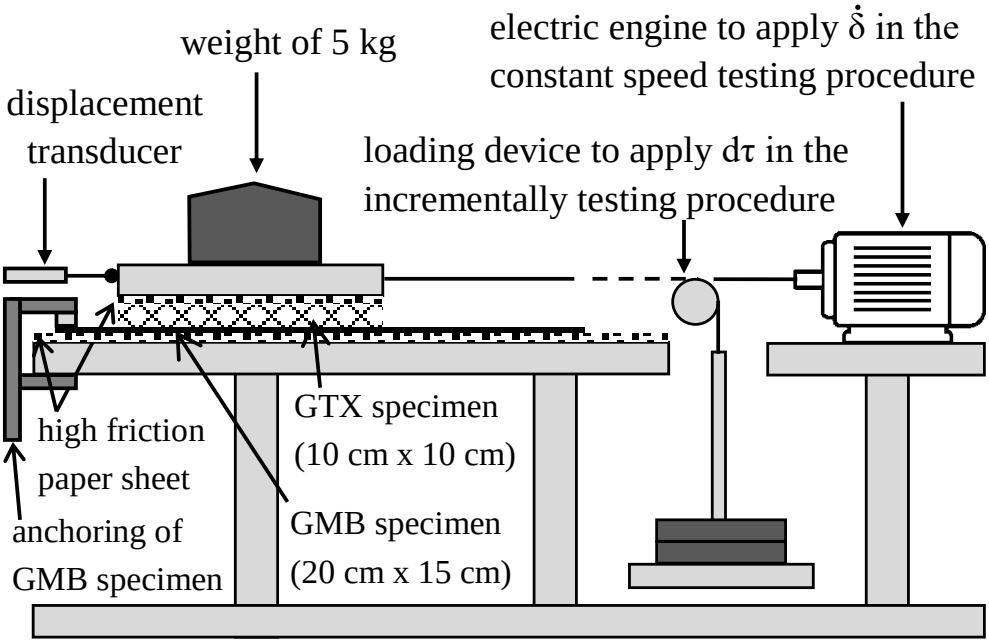

Figures 5. Results of the large-scale IP test following EN ISO 12957-2 of the four GMB-GTX$_{nw}$ interfaces: (a) relative displacement at the interface as a function of plane inclination and (b) sliding speed at the interface as a function of plane inclination.

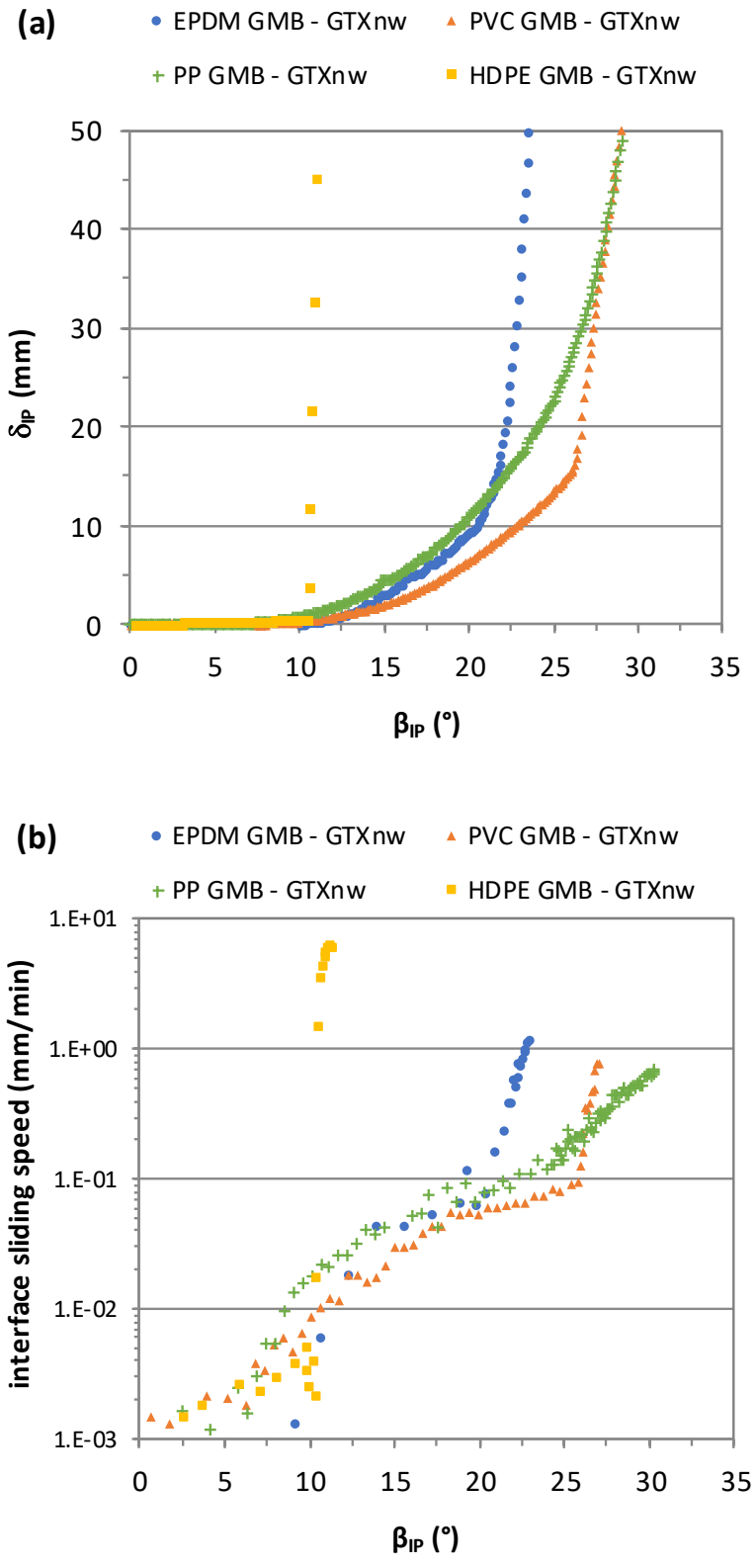

Figure 6. Results of large-scale IP tests of the four GMB-GTX$_{nw}$ interfaces. Tests were done following the incremental testing procedure (1° plane inclination per hour).

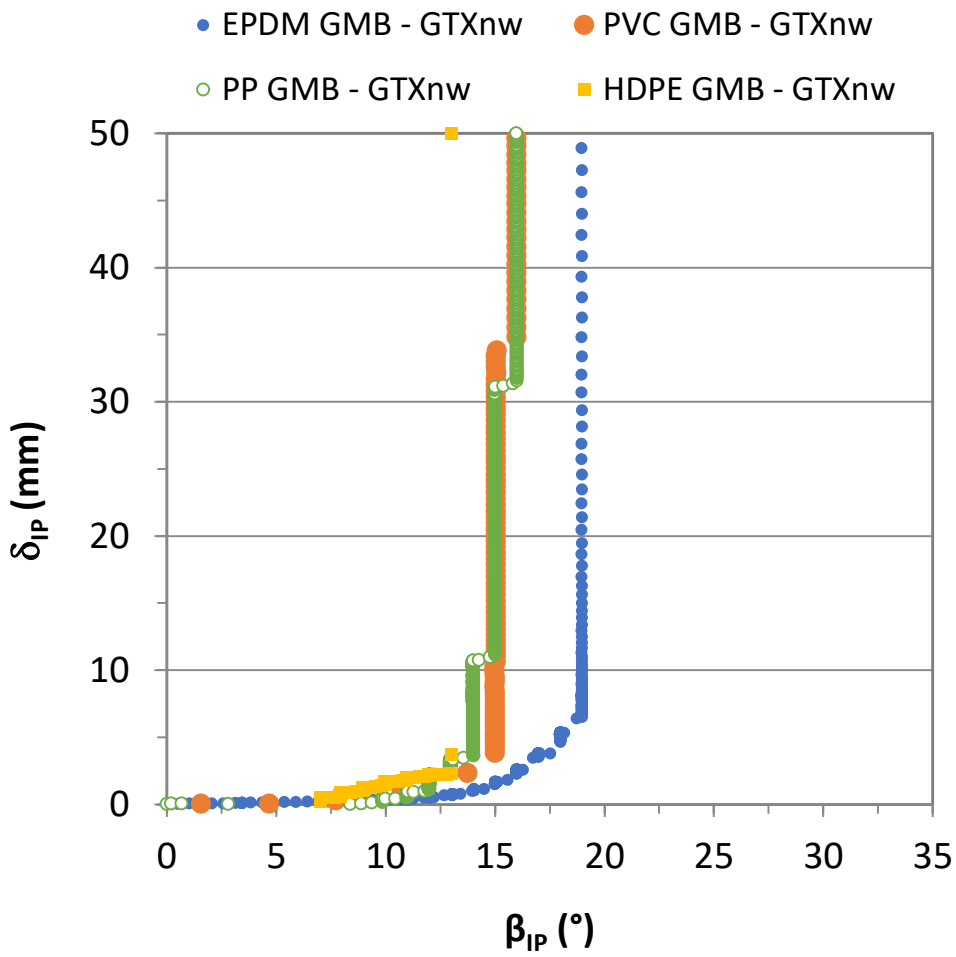

Figure 7. Relative displacement and sliding speed at the interface as a function of time, as obtained from large-scale IP tests done by applying the incremental testing procedure (1° plane inclination per hour) to the HDPE-GTX$_{nw}$ interface.

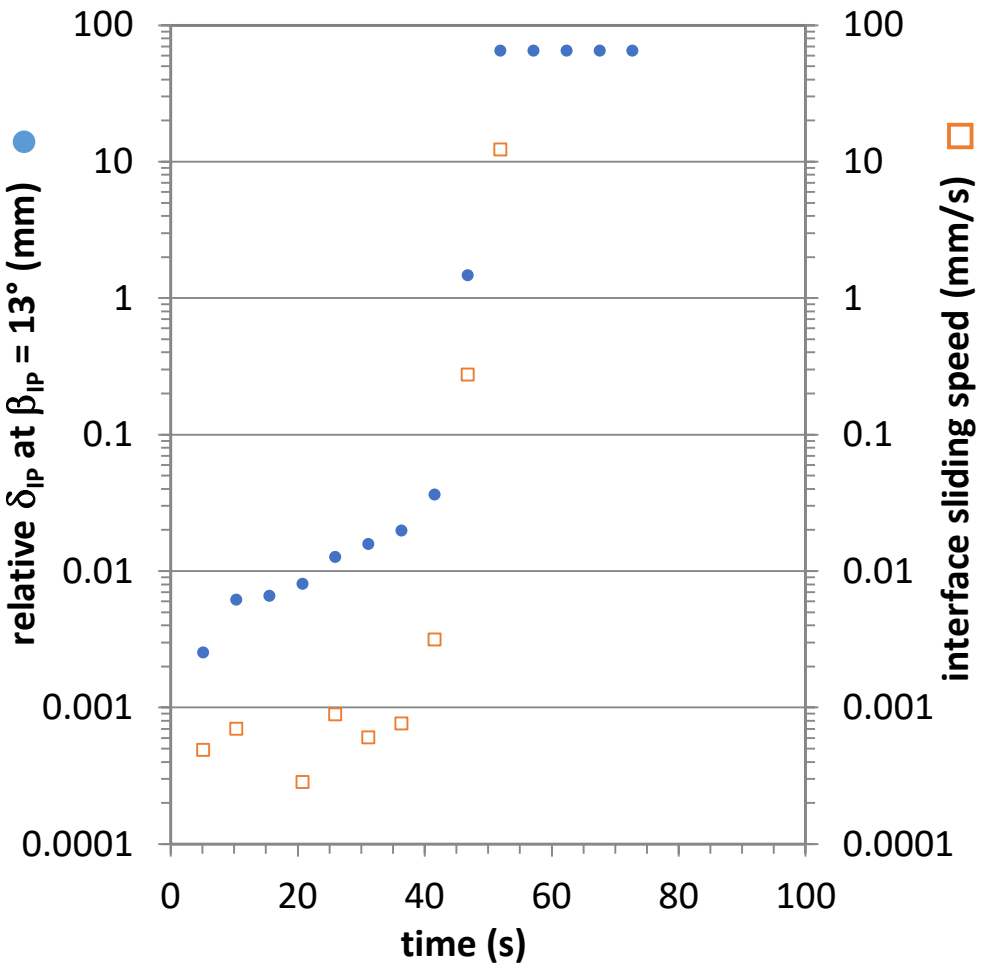

Figure 8. Relative displacement and sliding speed at the interface as a function of time, as obtained from large-scale IP tests done by applying the incremental testing procedure (1° plane inclination per hour) to the EPDM-GTX$_{nw}$ interface.

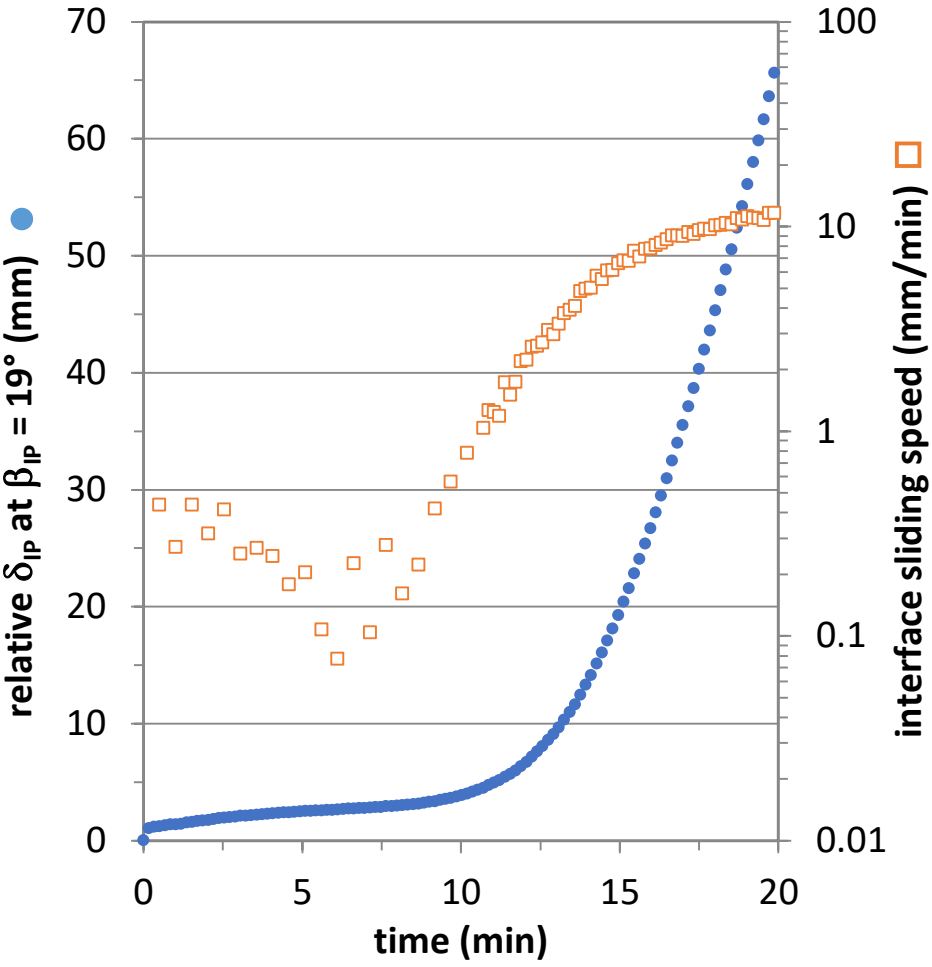

Figure 9. Relative displacement at the interface as a function of time obtained from large-scale IP tests done by applying the incremental testing procedure (1° plane inclination per hour) to the PVC GMB -GTX_{nw} interface.

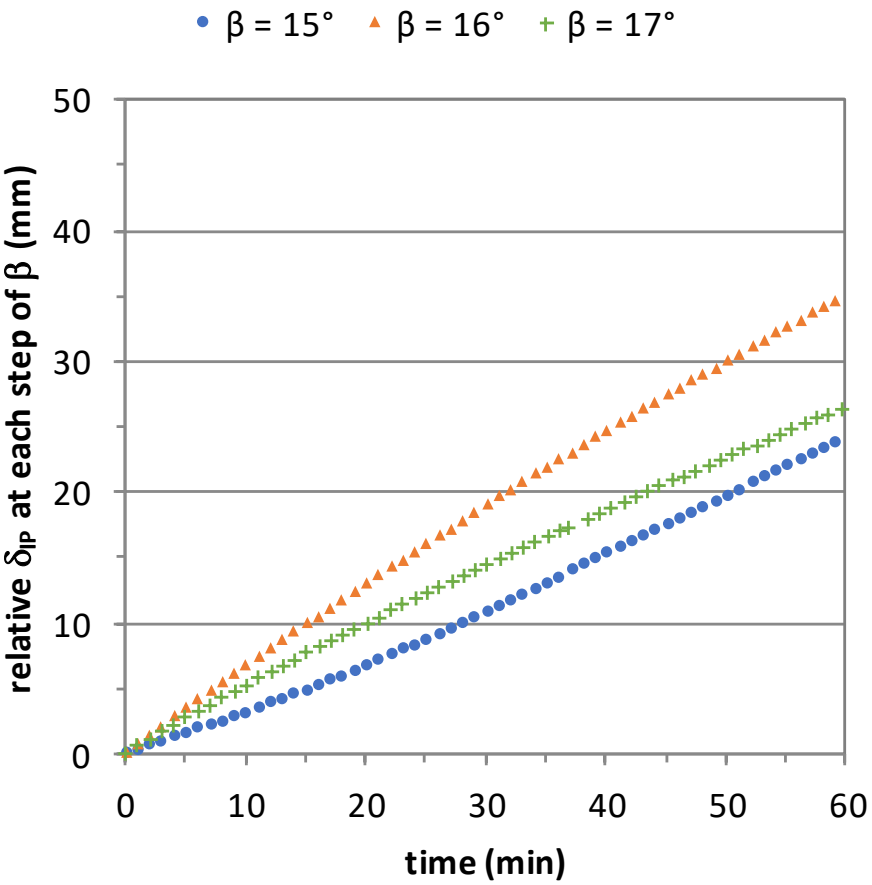

Figure 10. Results of large-scale IP test done by applying the incremental testing procedure (1° plane inclination per hour) to the PP-GTX$_{nw}$ interface: (a) relative displacement at the interface as a function of time and (b) sliding speed at the interface as a function of plane inclination.

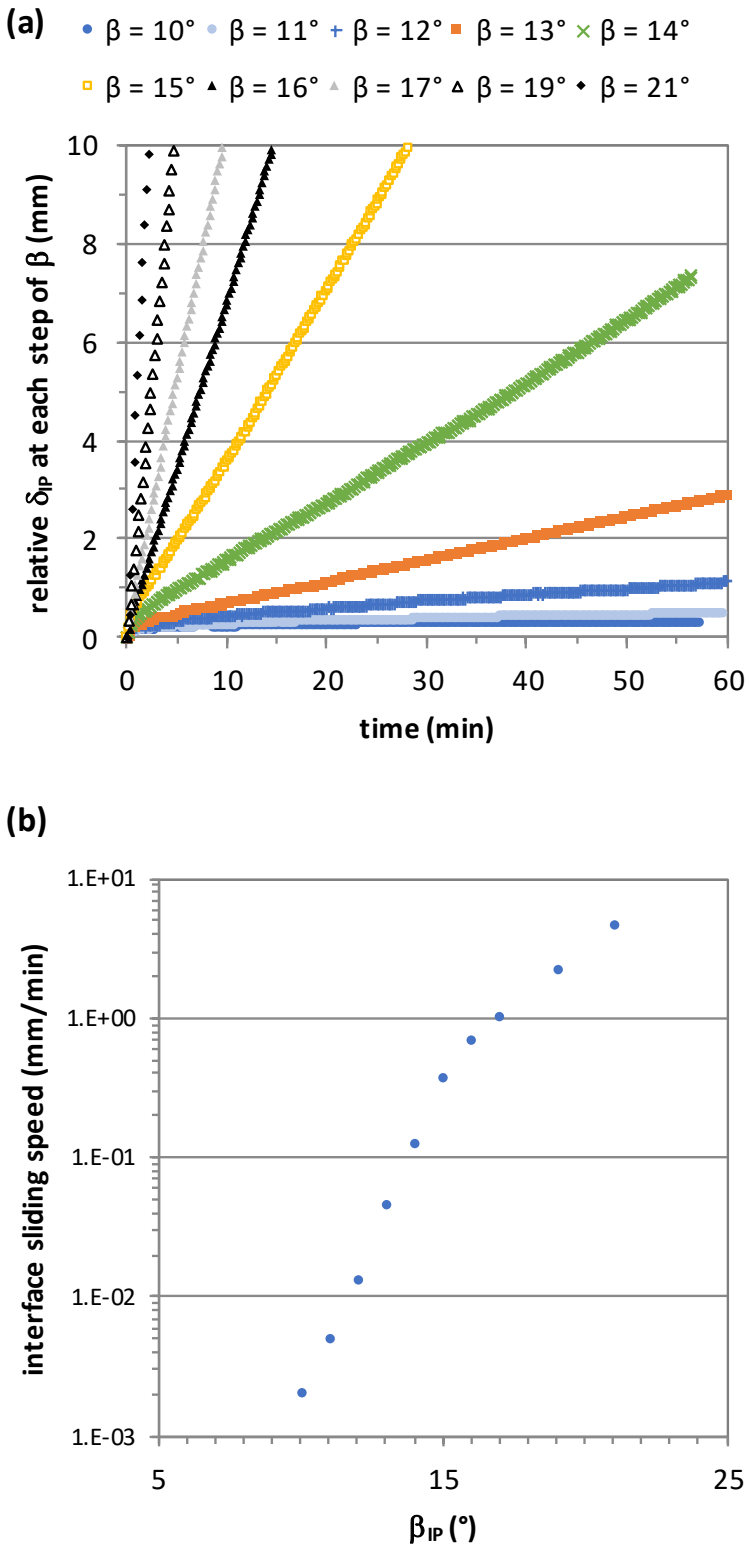

Figure 11. Results from large-scale SB tests of the PP GMB-GTX$_{nw}$ interface following the standard EN ISO 12957-1 at speeds of 1 and 0.1 mm/min: (a) shear curves (δ_{SB}, τ_{SB}) and (b) corresponding best fit regression straight line in the (σ_n, τ) diagram

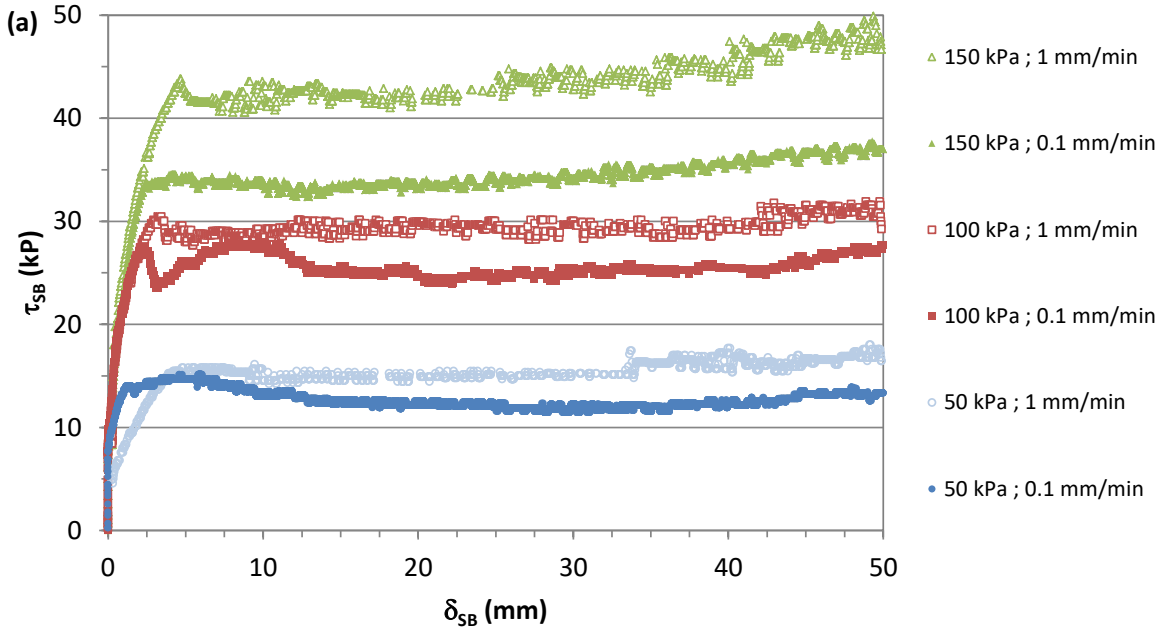

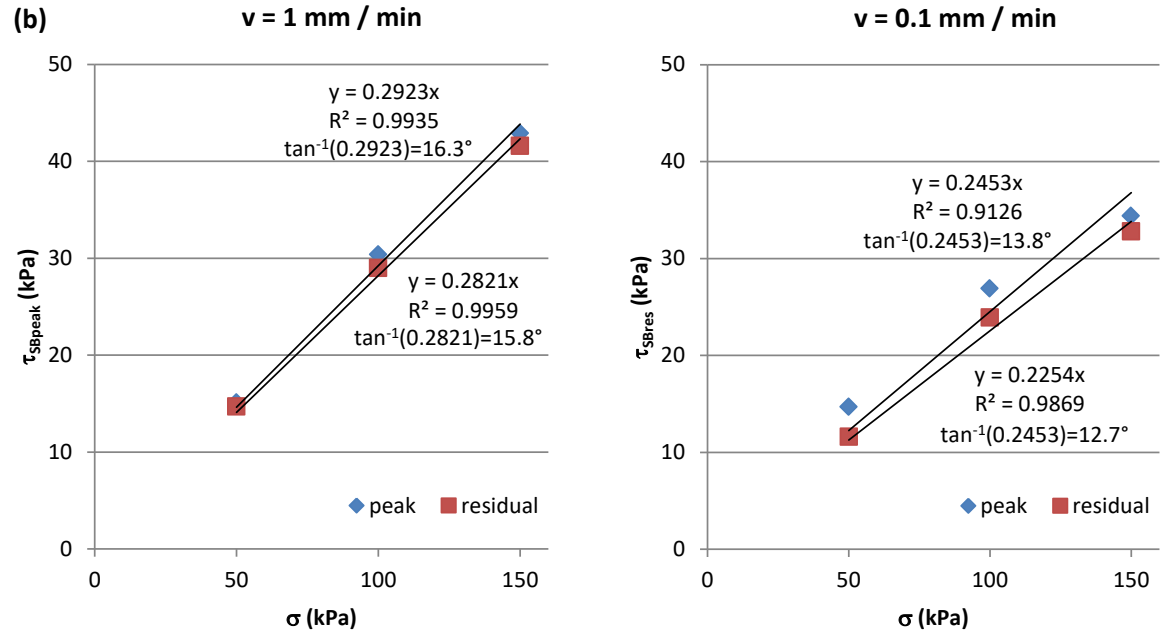

Figure 12. Results from ssSD test done by applying the incremental testing procedure to the PP GMB-GTX$_{nw}$ interface.

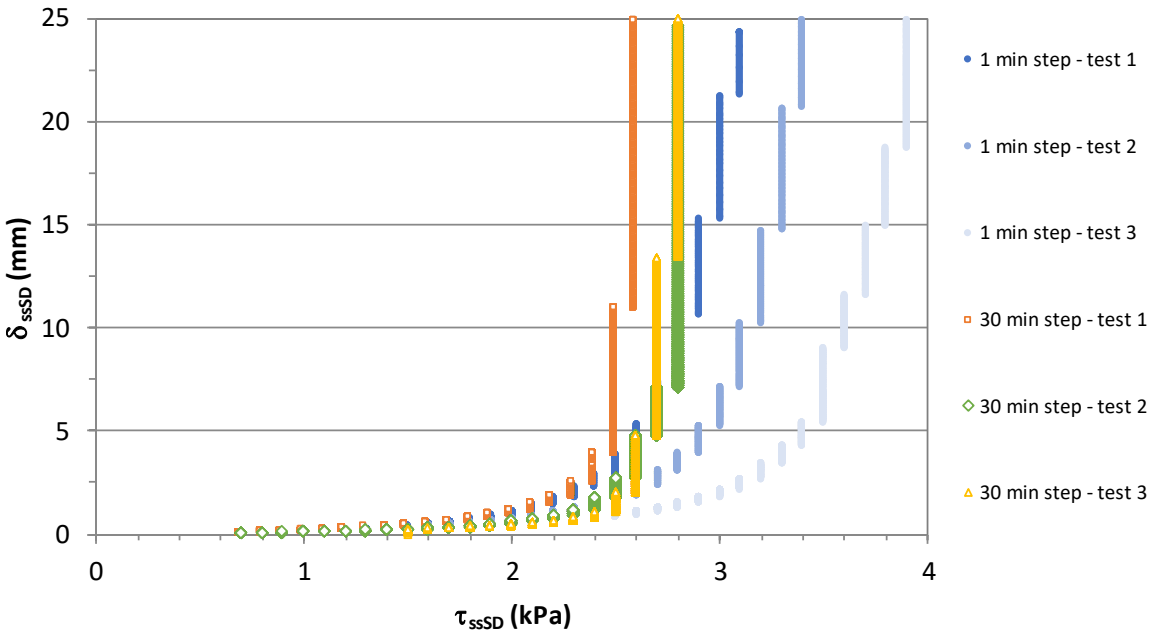

Figure 13. Results from ssSD test done by applying the testing procedure involving constant speed at the PP GMB-GTX$_{nw}$ interface.

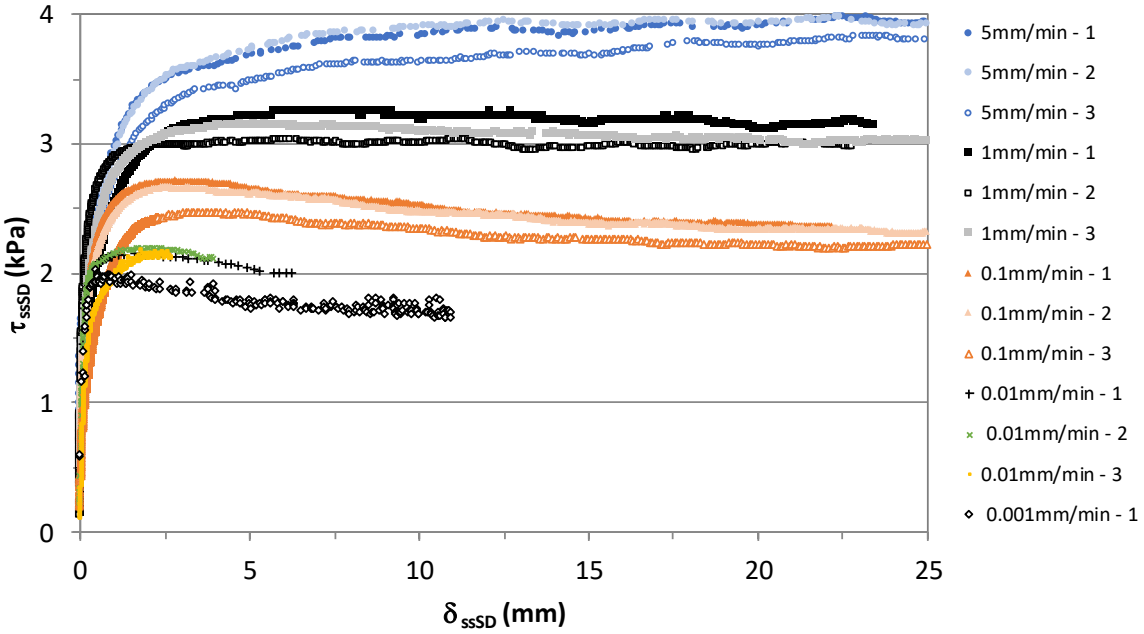

Figure 14. Sliding speed as a function of interface shear stress obtained from ssSD test done by applying both the incremental and constant-speed procedures at the PP GMB-GTX$_{nw}$ interface.

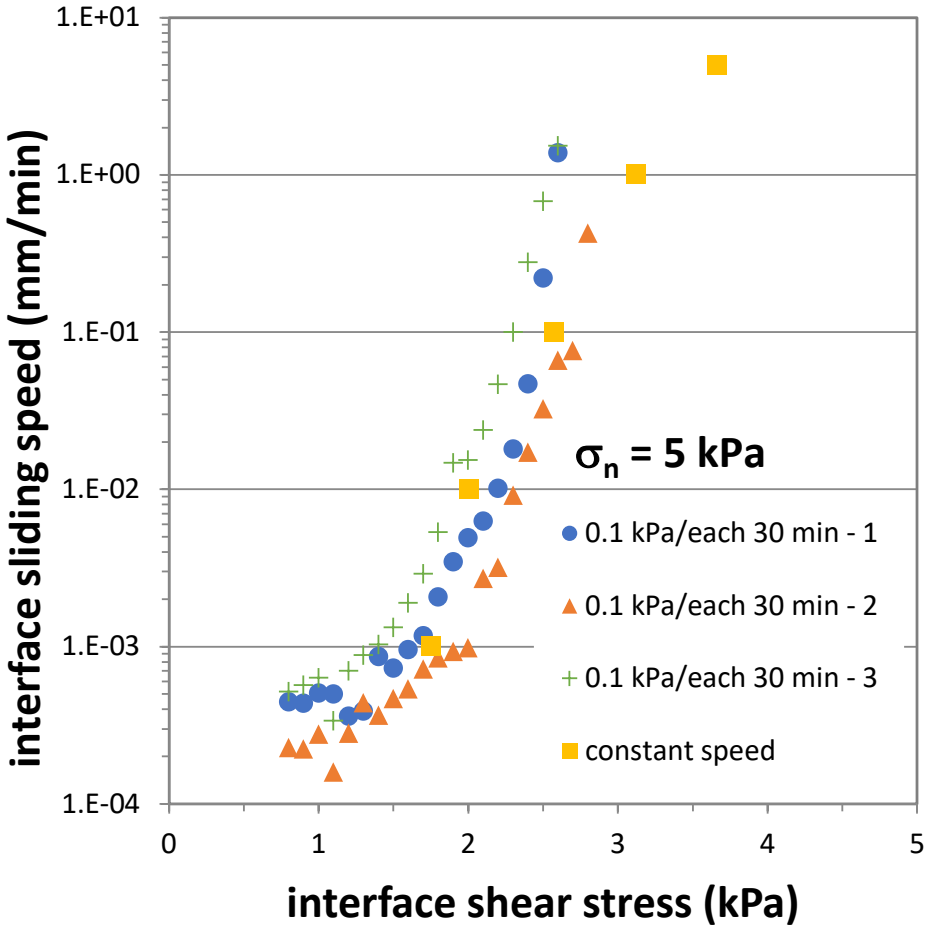

Figure 15. Effect of successive episodes of sliding at the PP GMB-GTX$_{nw}$ interface resulting from ssSD tests done both by (a) incrementally increasing the shear stress at the interface (0.1 kPa per 15 min) and by (b) imposing a constant tangential velocity at the interface (1 mm/min).

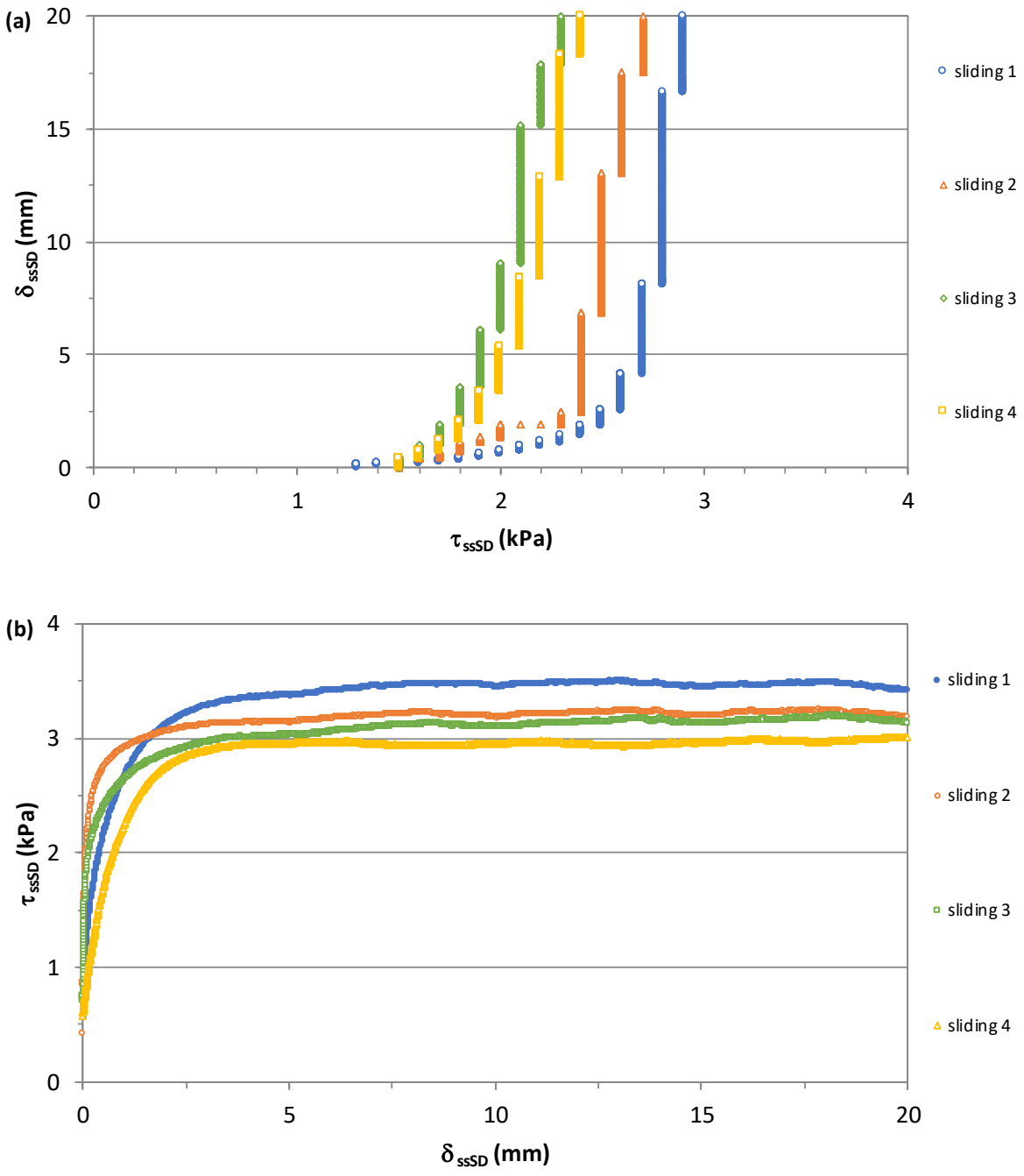

Figure 16. Effect of successive episodes of sliding at PP GMB-GTX$_{nw}$ interface resulting from ssSD tests done by imposing a constant velocity (1 mm/min) at the interface for (a) a single geomembrane specimen with four geotextile specimens, and (b) a single geotextile specimen with four geomembrane specimens.

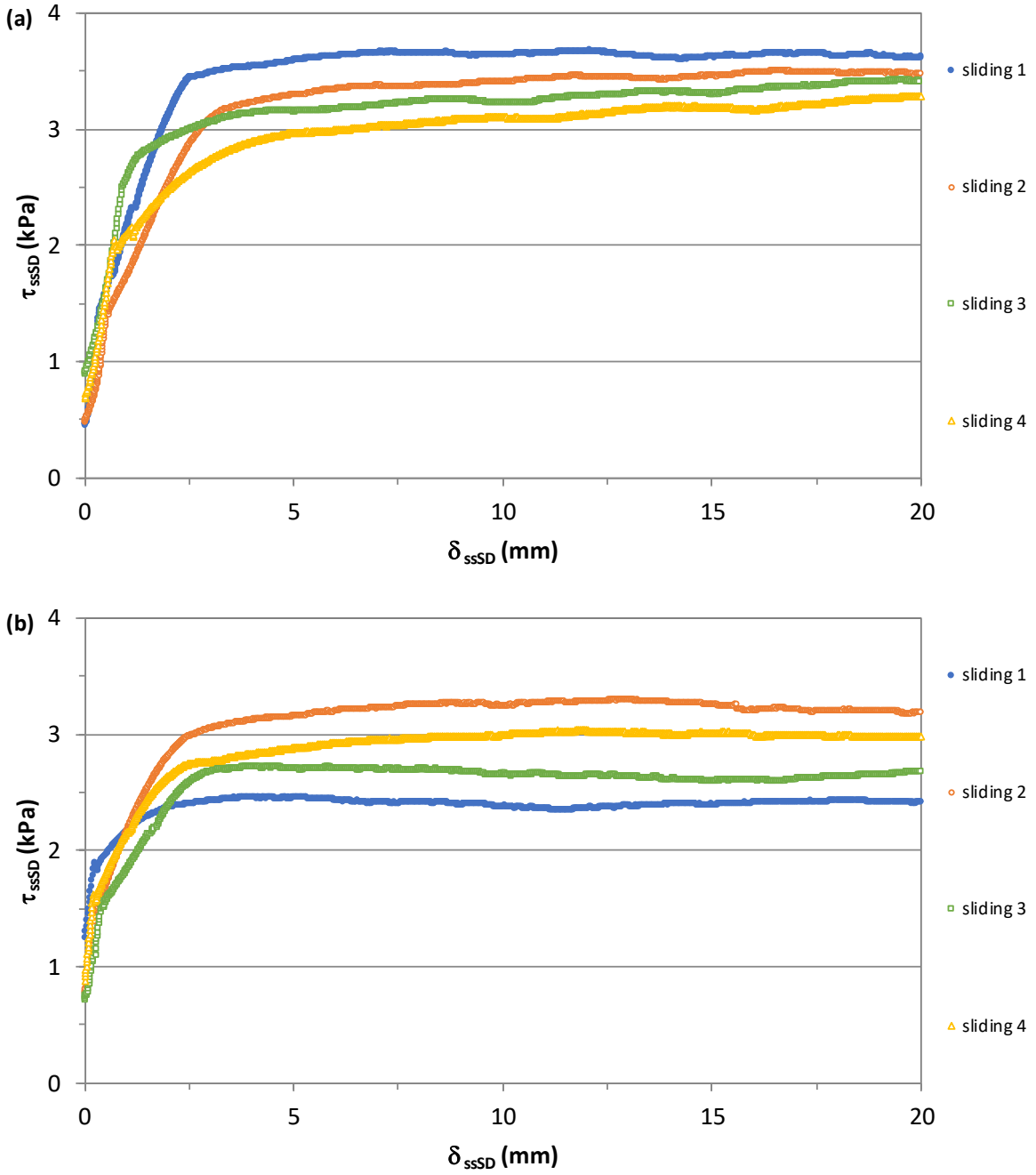

Figure 17. Results of large-scale IP tests done by incremental inclination of the PP-GTXnw interface (1° of plane inclination per 24 hours): (a) interface relative displacement as a function of plane inclination, and (b) interface relative displacement as a function of time.

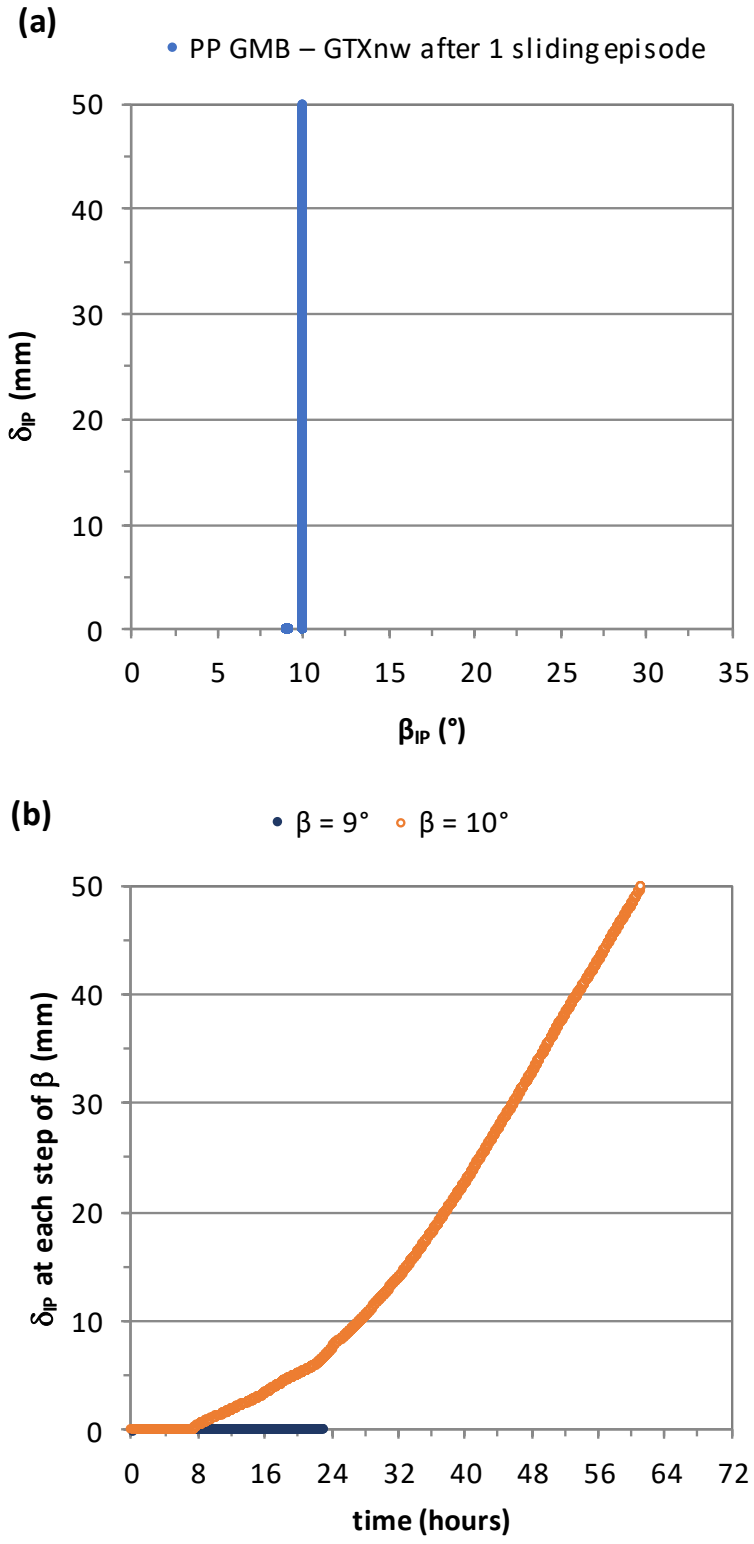

Table 1. Summary of main physical properties of geosynthetics.

Name in this study	Type	Nature	Structure/texture	Thickness (mm)	Mass per unit area (g/m²)
EPDM GMB	geomembrane	EPDM	Smooth	1.1	1329
HDPE GMB	geomembrane	HDPE	Smooth	2.0	1904
PP GMB	geomembrane	PP	Smooth	1.2	1095
PVC GMB	geomembrane	PVC	Smooth	2.2	2647
GTX_{nw}	geotextile	non-woven, PP	Needle-punched, short fibers	6.3	736

Table 2. Friction angles obtained following various testing procedures applied in the large-scale IP device.

Testing device	Large-scale IP (σ_o = 5 kPa)			
Testing procedure	following EN ISO 12957-2		incremental loading 1° per hour	incremental loading 1° per 24 hours after 1 sliding episode
Friction angle	interface angle (±0.2°) at β_{is} (δ=1mm) (failure possibly not reached)	standardised friction angle (±0.2°) at β_{50} (δ=50mm)	friction angle (±0.7°) at failure (unstabilised sliding)	friction angle (±0.7°) at failure (unstabilised sliding)
HDPE GMB/GTX_{nw}	14.0	14.7	16.7	na
EPDM GMB/GTX_{nw}	17.3	31.1	24.7	na
PVC GMB/GTX_{nw}	16.7	36.8	19.3	na
PP GMB/GTX_{nw}	14.0	37.6	na	12.9

Table 3. Ratio of shear stresses of the PP GMB/GTX_{nw} interface tested with the small-scale SD and large-scale SB at various normal stresses and tangential velocities

	Small-scale SB (σ_n = 5 kPa)	Large-scale SB ($50 \leq \sigma_n \leq 150$ kPa)		
normal stress σ_n (kPa)	5	50	100	150
(τ at δ = 5 mm for v = 0.1 mm/min) / (τ at δ = 5 mm v = 1 mm/min)	0.82	0.97	0.93	0.80
(τ at δ = 20 mm for v = 0.1 mm/min) / (τ at δ = 20 mm v = 1 mm/min)	0.76	0.82	0.82	0.78